ARMY RESEARCH LABORATORY

Transmitted Reference Ultra Wideband Transceivers For Multiuser Communication

by Zhengyuan Xu and Brian M. Sadler

ARL-TR-3708 **January 2006**

Approved for public release; distribution unlimited.

NOTICES

Disclaimers

The findings in this report are not to be construed as an official Department of the Army position unless so designated by other authorized documents.

Citation of manufacturer's or trade names does not constitute an official endorsement or approval of the use thereof.

Destroy this report when it is no longer needed. Do not return it to the originator.

Army Research Laboratory
Adelphi, MD 20783-1197

ARL-TR-3708 **January 2006**

Transmitted Reference Ultra Wideband Transceivers For Multiuser Communication

Zhengyuan Xu and Brian M. Sadler
Computational and Information Sciences Directorate, ARL

Approved for public release; distribution unlimited.

REPORT DOCUMENTATION PAGE

Form Approved
OMB No. 0704-0188

Public reporting burden for this collection of information is estimated to average 1 hour per response, including the time for reviewing instructions, searching existing data sources, gathering and maintaining the data needed, and completing and reviewing the collection information. Send comments regarding this burden estimate or any other aspect of this collection of information, including suggestions for reducing the burden, to Department of Defense, Washington Headquarters Services, Directorate for Information Operations and Reports (0704-0188), 1215 Jefferson Davis Highway, Suite 1204, Arlington, VA 22202-4302. Respondents should be aware that notwithstanding any other provision of law, no person shall be subject to any penalty for failing to comply with a collection of information if it does not display a currently valid OMB control number.
PLEASE DO NOT RETURN YOUR FORM TO THE ABOVE ADDRESS.

1. REPORT DATE *(DD-MM-YYYY)*	2. REPORT TYPE	3. DATES COVERED (From - To)
January 2006	Summary	FY05

4. TITLE AND SUBTITLE
Transmitted Reference Ultra Wideband Transceivers for Multiuser Communication

5a. CONTRACT NUMBER

5b. GRANT NUMBER

5c. PROGRAM ELEMENT NUMBER

6. AUTHOR(S)
Zhengyuan Xu and Brian M. Sadler

5d. PROJECT NUMBER

5e. TASK NUMBER

5f. WORK UNIT NUMBER

7. PERFORMING ORGANIZATION NAME(S) AND ADDRESS(ES)
U.S. Army Research Laboratory
ATTN: AMSRD-ARL-CI-CN
2800 Powder Mill Road
Adelphi, MD 20783-1197

8. PERFORMING ORGANIZATION REPORT NUMBER
ARL-TR-3708

9. SPONSORING/MONITORING AGENCY NAME(S) AND ADDRESS(ES)
U.S. Army Research Laboratory
2800 Powder Mill Road
Adelphi, MD 20783-1197

10. SPONSOR/MONITOR'S ACRONYM(S)

11. SPONSOR/MONITOR'S REPORT NUMBER(S)

12. DISTRIBUTION/AVAILABILITY STATEMENT
Approved for public release; distribution unlimited.

13. SUPPLEMENTARY NOTES

14. ABSTRACT
A conventional transmitted reference (TR) modulation scheme is an effective means to combat severe multipath distortion in an ultra wideband (UWB) system, significantly relaxing the equalization requirements at a cost in performance. However, it suffers from multiple access and other interference, and a rate loss of 50%. In this paper we extend TR modulation to the multiuser case, while boosting data transmission to near full rate. To enable multiple access, the proposed multiuser TR (MTR) scheme assigns a pair of frame rate pseudo-random (PN) sequences to each user, modulating the amplitude of each of two consecutive pulses, respectively.
Given a user's reference-pulse modulating PN sequence, mean-based estimation is proposed to obtain a clean waveform template, which is appropriate for both pulse-amplitude (PAM) or pulse-position modulation (PPM).
Along with interference reduction, this method enables arbitrarily small spacing of pulse pairs, leading to near full rate transmission. Using the waveform template and the data-pulse modulating PN sequence, any reference pulse interference is subtracted and data demodulation carried out. Aided by the PN sequences, the proposed estimation and data detection scheme is able to mitigate both inter-pulse and multi-access interference. To further reduce interference a time-hopping code can also be employed. Waveform estimation and bit error rate analysis are provided for the multi-user case, and confirmed with simulations. Substantial detection improvements over conventional TR detectors are observed.

15. SUBJECT TERMS
Ultra wideband, transmitted reference, full rate, increased capacity, inter-pulse interference, multiple access

16. SECURITY CLASSIFICATION OF:			17. LIMITATION OF ABSTRACT	18. NUMBER OF PAGES	19a. NAME OF RESPONSIBLE PERSON
a. REPORT	b. ABSTRACT	c. THIS PAGE			Brian M. Sadler
Unclassified	Unclassified	Unclassified	UL	42	19b. TELEPHONE NUMBER (*Include area code*) (301) 394-1239

Standard Form 298 (Rev. 8/98)
Prescribed by ANSI Std. Z39.18

Contents

List of Figures

1 Introduction

The approval of ultra-wideband (UWB) transmission in the United States [1] and elsewhere has sparked significant research interest [2], [3], [4]. Potential applications include not only short-range data and multimedia communications, but also sensing, localization and tracking, as well as collision avoidance and other radar-like scenarios. UWB offers unique features such as high resolvability of multiple paths, fine timing resolution [5], and coexistence via overlay with existing wireless systems [6].

However, UWB communication systems must somehow accommodate the significant channel distortion, and a full accounting requires very high receiver complexity. Generally, UWB receivers sacrifice performance for lowered complexity [7], [8]. Categories include the threshold detector [8], [9], RAKE receiver [5], [10], [11], [12], and autocorrelation receiver [13], [14], [15]. A practical RAKE receiver consists of multiple correlators [10]. It must select a moderate yet limited number of strong paths to combine from dozens to hundreds of possible paths. Despite medium complexity, captured energy may be relatively low and is very sensitive to delay selection. The RAKE also suffers from channel (time of arrival and attenuation) mismatch although high rate sampling helps to estimate channel coefficients in the design of linear receivers [16], [17].

Transmitted reference (TR) modulation appears as an effective means to mitigate multipath distortion in a UWB communication system [18], [19], [20], [21]. TR was proposed for narrowband systems a few decades ago [22], [23], [24]. The first pulse of each doublet is information-free, and the second (delayed) pulse carries the user's information via binary phase shift keying (BPSK), pulse amplitude modulation (PAM), or pulse position modulation (PPM). The delay of the data pulse is ideally designed to be larger than the channel spread such that the reference pulse does not interfere with the data pulse after multipath propagation (no inter-pulse interference - IPI), although this may be difficult to achieve in an analog delay implementation. The received waveform resulting from the reference pulse can then serve as a template to demodulate the latter data pulse using a low complexity correlation receiver [20], [25]. However, minimum spacing of the two pulses inevitably sacrifices data rate, especially when the channel delay spread is large [26]. As the channel is used only half the time for data at best, there is a 50% rate penalty. In addition, the template may be very noisy, limiting the conventional TR performance. If small spacing between pulses is incorporated in order to increase the transmission rate, then IPI contaminates the template and may consequently yield poor detection performance.

In order to improve template estimation with PAM modulation, [20] and [25] propose to average signals from multiple frames within one symbol interval to minimize the noise effect. Consequently, better detection performance is achieved than a conventional receiver

built upon an instantaneous estimate of the template. To obtain a clean template for either PAM or PPM modulation based systems, the noise effect can be further alleviated by statistically averaging signals over multiple symbol intervals [27]. The signal waveform estimator utilizes the first order statistic of the received signals. For PAM signaling, the estimated signal waveform directly serves as a template for data detection, while for PPM signaling, a template is constructed based on that estimate. Contrary to all previous TR schemes, no requirement on large pulse spacing at the transmitter is imposed, enabling near full rate data transmission. The mutual interference (IPI) between the reference and data signal at the receiver can be effectively mitigated. During waveform estimation, IPI from the data pulse is tackled by taking into account the input distribution, yielding a more purified template. During detection, IPI from the reference pulse can be subtracted after the reference signal is estimated. At high SNR the waveform estimation mean square error (MSE) decreases in proportion to the number of observation windows, and the MSE is significantly smaller than those from existing methods and the conventional TR scheme. Consequently, detection based on the improved template shows significant performance gain. This gain is slightly better for PAM than for PPM, in terms of both MSE and bit error rate (BER) [27].

In this paper we build on the above ideas, expanding to a multiuser scenario. The proposed multiuser TR (MTR) scheme incorporates psuedo-random coding, similar to that in [28], [29] borrowed from an overlaying code division multiple access (CDMA) system [30], [31]. Since both reference and data pulses need to be differentiated across users in order to easily estimate the desired user's waveform and demodulate its data, two pseudo-random (PN) sequences are assigned to each user at the frame rate. The first spreading sequence is used to modulate the amplitude of the reference pulse, while the second one is applied to the data pulse. A mean-based estimation algorithm is proposed to obtain an enhanced signal waveform template for either PAM or PPM based UWB systems. Arbitrarily small spacing between reference and data pulses is enabled, leading to near full rate transmission. Assisted by the waveform template for the desired user, and the PN sequence modulating its data pulse, the interfering contribution from its reference pulse is subtracted before demodulation. Reference signals from all users can be suppressed if their PN sequences are known and signal waveforms estimated, such as in uplink communication to an access point initiated by different users/nodes. The proposed estimation and data detection schemes are able to mitigate both IPI and multiple access interference (MAI) mainly due to the pseudo-random sequence properties. In order to enhance the interference mitigation capability of the proposed systems, a time hopping sequence may be applied to the data pulse of each user. The waveform estimator requires only delay elements, adders, and multipliers, while the correlation receiver performs addition, integration, and symbol rate sampling operations. Thus implementation is possible in mixed analog/digital circuitry. Waveform estimation MSE, and BER detection performance, are developed analytically and studied via simulation using the IEEE UWB

channel models [33]. Effects of observation window size, signal to noise ratio (SNR), number of users, signal to interference ratio, and channel models are investigated in detail. Substantial detection improvements over conventional detectors are observed.

The paper is organized as follows. First, in section 2, the proposed MTR transmission schemes and data models are developed for both PAM and PPM. The corresponding waveform estimation and detection methods are described in section 3. In section 4 we analyze the estimation and detection in detail. Our study covers various scenarios including PAM and PPM modulations, as well as downlink and uplink communications exploiting knowledge of the desired user PN code, or all users codes, respectively. For concise presentation of analytical results, several notational definitions are introduced. Numerical examples are shown in section 5 and key contributions of the work are summarized in the conclusions.

2 Near Full-Rate MTR-UWB Systems

A conventional TR UWB system considers single user transmission [19]. A user transmits a doublet in each frame of T_f seconds. The first pulse serves as a reference and is information free. The second pulse is data modulated by either PAM or PPM and delayed by τ seconds. Denote the pulse by $w(t)$ with duration T_w. Assume each symbol repeats N_f frames, so the symbol period is $T_s = N_f T_f$. In order to accommodate multiuser communication, a MTR UWB scheme is necessary. We propose to associate a unique covering PN sequence with the reference pulse at the frame rate. That PN sequence will be used for estimation of signal waveform that is subsequently used as a template by a correlation detector. Meanwhile, the other covering PN sequence is employed to randomize the data modulated pulse, and reduce waveform estimation error and MAI. These two PN sequences together uniquely specify a user. They also help to increase the system capacity, as in a CDMA system [30], [31]. In a multiuser environment, delay of the second pulse is controlled by another user-dependent time hopping sequence to further minimize MAI. It will be revealed that this delay can be arbitrarily small to achieve near full rate transmission, contrary to a conventional TR system that typically sets it to be large enough to avoid IPI at the receiver [18]. In the proposed transmission scheme, data modulation can be either PAM or PPM [18], [20]. For easy illustration of the proposed transmission, estimation, and detection schemes, binary PAM or PPM modulation is assumed, although it is straightforward to generalize the models and methods to high order modulations.

2.1 PAM Signaling

Denote the n-th binary PAM symbol of user k in a K-user UWB system by $I_{k,n} \in \{\pm 1\}$. Transmitted signal with power $\mathcal{P}_k$ from user k can be described by

$$s_k(t) = \sqrt{\frac{\mathcal{P}_k}{2}} \sum_{n=-\infty}^{\infty} \Big[A_{k,n} w(t - nT_f) + I_{k,\lfloor n/N_f \rfloor} B_{k,n} w(t - nT_f - \tau_{k,n}) \Big], \tag{1}$$

where $A_{k,n}$ and $B_{k,n}$ are frame-rate binary PN sequences taking values ± 1. They can also be chosen randomly from a ternary set $\{+1, 0, -1\}$ with pre-specified probabilities, providing more flexibility to MAI rejection and multipath mitigation [32]. Notation $\lfloor \cdot \rfloor$ is an integer floor operator. Delay $\tau_{k,n} = c_{k,n} T_c$ of the second pulse is designed to minimize MAI as well where $c_{k,n} \in \{D, D+1, \cdots, D_{max}\}$ is the hopping code, T_c is the chip duration, $T_f = N_c T_c$. A block diagram of a typical transmitter is presented in Figure 1. The minimum spacing of two pulses is $T_d \triangleq D T_c$. It can be arbitrarily small under a mild $T_d > T_w$ requirement to achieve near full rate data transmission. It thus eliminates a 50% rate penalty, similar to single-user modeling without PN coding [27]. Therefore, signals resulting from reference and data pulses after multipath propagation may severely interfere with each other, causing IPI. If we denote a multipath channel impulse response by $\theta_k(t)$, and transmitter-receiver front end bandpass filter by $g(t)$, the received signal becomes

$$r(t) = \sum_{k=1}^{K} \sum_{n=-\infty}^{\infty} \Big[A_{k,n} h_k(t - nT_f) + I_{k,\lfloor n/N_f \rfloor} B_{k,n} h_k(t - nT_f - c_{k,n} T_c) \Big] + v(t), \tag{2}$$

where $h_k(t) = \sqrt{\frac{\mathcal{P}_k}{2}} w(t) \star \theta_k(t) \star g(t)$ is the unknown waveform, $\star$ denotes convolution, $v(t) = n(t) \star g(t)$ and $n(t)$ represents zero mean Gaussian noise with two-sided power spectral density $\frac{N_0}{2}$. Propagation delay for each user is ignored for simplicity, but is analytically unnecessary. Indeed, it creates the worst communication scenario when other users maximally interfere with the desired user. Generally, MAI may be reduced if the users signals are mis-aligned. This simple reasoning suggests the worst-case detection performance (BER upper bound) based on this model. Even in this case, our analysis of the proposed methods is lengthy. Suppose all $h_k(t)$ have support in $(0, T_h)$. Since both reference and data pulses propagate through the same channel, $h_k(t)$ is not only the received signal due to the reference pulse, but also the waveform of the data symbol after delay $\tau_{k,n}$. Though technically unnecessary, assume $T_h + \tau_{k,n} < T_f$ for simplified analysis of the methods proposed later. Discussions can be easily generalized to other situations. Even so however, severe IPI results. Hence if $h_k(t)$ is directly used as a template for a correlation receiver as in a conventional TR system, it leads to a large data demodulation error.

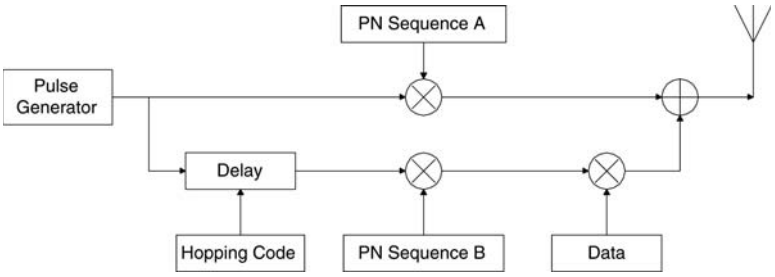

Figure 1: Block diagram of the MTR-UWB transmitter.

Therefore, a mean-based estimation technique will be proposed to clean the "dirty" template based on an observation window spanning multiple symbol intervals. The model reduces to a conventional TR system if $K = 1$, $A_{k,n}$ and $B_{k,n}$ take values 1, and delay $\tau_{k,n}$ is set as T_d. $B_{k,n}$ can still be introduced to a subsequently improved single-user system [27] to reduce waveform estimation error. Though technically unnecessary, assume $T_h + \tau_{k,n} < T_f$ for simplified analysis of the methods proposed later. Discussions can be easily generalized to other situations. Even so however, severe IPI results. Hence if $h_k(t)$ is directly used as a template for a correlation receiver as in a conventional TR system, it leads to a large data demodulation error. Therefore, a mean-based estimation technique will be proposed to clean the "dirty" template based on an observation window spanning multiple symbol intervals. The model reduces to a conventional TR system if $K = 1$, $A_{k,n}$ and $B_{k,n}$ take values 1, and delay $\tau_{k,n}$ is set as T_d. $B_{k,n}$ can still be introduced to a subsequently improved single-user system [27] to reduce waveform estimation error.

2.2 PPM Signaling

A PPM transmitter block diagram similar to figure 1 can be drawn by replacing corresponding data modulation and delay control. Similarly, after propagating through a multipath channel, the received signal has the following form

$$r(t) = \sum_{k=1}^{K} \sum_{n=-\infty}^{\infty} \left[A_{k,n} h_k(t - nT_f) + B_{k,n} h_k(t - nT_f - c_{k,n} T_c - \tau_{I_{k,\lfloor n/N_f \rfloor}}) \right] + v(t), \quad (3)$$

where $h_k(t)$ is the waveform including the transmitted pulse, multipath channel, and filter, and $\tau_{I_{k,n}} = I_{k,n}\sigma_d$ is the delay controlled by a binary information sequence $I_{k,n}$ that takes $\{0, 1\}$ with equal probability. If modulation parameter σ_d is related to T_c by $\sigma_d = \alpha T_c$, then α can be designed to optimize the detection performance [7].

Our goal is to detect information sequence $I_{k,n}$ in the unknown channel for either PAM or PPM modulation based UWB systems according to the proposed model (2) or (3)

respectively. First, the signal waveform $h_k(t)$ will be estimated from received signal $r(t)$. This will serve as a template to detect the PAM symbol (or used to construct a template to detect the PPM symbol), via a correlation detector [7], [20].

3 Template Acquisition and Symbol Detection

In a conventional TR system, a detection process involves acquisition of a template first and then correlation detection based on that template. The template is directly taken from the reference pulse (the first term in each model). Thus signal $r(t)$ in the first segment of that frame is used as a template to correlate with $r(t)$ in the second segment for PAM signaling, or used to construct a template to detect the PPM symbol. As is known, such a template is very noisy even in a single user system. In [25], averaging of $r(t)$ over N_f frames within one symbol period is performed to reduce noise. In a multiuser system, it is observed that $h_k(t)$ is corrupted by reference signals of other users, all users' data pulses, and background noise. Thus the conventional detection method will yield a very "dirty" template and consequently cause large detection errors. However, exploiting the PN sequences and zero mean property of the noise, statistical averaging of segments of $r(t)$ (normalized by $A_{k,n}$) from different frames across multiple symbol intervals significantly reduces interference (even for the non-zero mean PPM symbol case). The interference reduction does not depend on the transmit pulse spacing.

Because of repetitive transmission of a reference pulse, each user's waveform $h_k(t)$ repeats from frame to frame. Therefore it is reasonable to partition the received signal $r(t)$ into segments, each of frame duration T_f, in order to estimate the waveform. Let's consider user k and estimate $h_k(t)$. Take $r(t)$ in N_s symbol intervals. There are a total of $N_p \triangleq N_f N_s$ segments. The m'-th ($m' = 1, \cdots, N_p$) segment of $r(t)$ is defined as $r_{m'}(t) \triangleq r(t + m'T_f)$ for $t \in [0, T_f)$, and $r_{m'}(t) \triangleq 0$ elsewhere. Similarly, define $v_{m'}(t)$ for the noise. For PAM signaling, according to (2) and assisted by the first PN sequence of this user that takes values ± 1, we find

$$A_{k,m'} r_{m'}(t) = h_k(t) + \sum_{l \neq k, l=1}^{K} A_{k,m'} A_{l,m'} h_l(t) + A_{k,m'} v_{m'}(t) + \sum_{l=1}^{K} A_{k,m'} B_{l,m'} I_{l,\lfloor m'/N_f \rfloor} h_l(t - c_{l,m'} T_c). \tag{4}$$

It is observed that this signal contains abundant interference from other users reference signals, noise, and all users data signals. Hence it is very noisy and not appropriate to be directly used as a template. However, after taking expectation, it becomes

$$E\{A_{k,m'}r_{m'}(t)\} = h_k(t) + \sum_{l\neq k,l=1}^{K} A_{k,m'}A_{l,m'}h_l(t), \tag{5}$$

because $E\{I_{l,\lfloor m'/N_f\rfloor}\} = 0$ and $E\{v_{m'}(t)\} = 0$. So, in the mean, interference is attributed to reference signals only. It can be further reduced after considering the PN property, as discussed below. For PPM signaling, using $A_{k,m}$ to extract the waveform from the m'-th segment of $r(t)$ in (3)

$$\begin{aligned} A_{k,m'}r_{m'}(t) &= h_k(t) + \sum_{l\neq k,l=1}^{K} A_{k,m'}A_{l,m'}h_l(t) + A_{k,m'}v_m(t) \\ &+ \sum_{l=1}^{K} A_{k,m'}B_{l,m'}h_l(t - c_{l,m'}T_c - \tau_{I_{l,\lfloor m'/N_f\rfloor}}). \end{aligned} \tag{6}$$

Its expected value is

$$E\{A_{k,m'}r_{m'}(t)\} = h_k(t) + \sum_{l\neq k,l=1}^{K} A_{k,m'}A_{l,m'}h_l(t) + \sum_{i=0}^{1}\sum_{l=1}^{K}\frac{1}{2}A_{k,m'}B_{l,m'}h_l(t - c_{l,m'}T_c - i\alpha T_c), \tag{7}$$

where expected value of the PPM modulated data pulse has been evaluated with equally probable values in $\{0, 1\}$, and modulation delay $\tau_{I_{k,\lfloor m'/N_f\rfloor}} = I_{k,\lfloor m/N_f\rfloor}\alpha T_c$. If high order PPM modulation is employed, then we can adapt the upper limit in the summation for i (and change probability $\frac{1}{2}$) in the above equation. Now interference stems from not only reference signals, but also data signals due to non-zero mean of all inputs, and these depend on the PN sequences. The time average of each of $A_{k,m'}A_{l,m'}$ and $A_{k,m'}B_{l,m'}$ over N_p frame intervals favorably approaches zero as N_p increases. Therefore, according to (5) and (7), an estimate of the waveform for a multiuser system (either PAM or PPM signaling) can be described along the lines of a single-user waveform estimator in [27] as follows The time average of each of $A_{k,m'}A_{l,m'}$ and $A_{k,m'}B_{l,m'}$ over N_p frame intervals favorably approaches zero as N_p increases. Therefore, according to (5) and (7), an estimate of the waveform for a multiuser system (either PAM or PPM signaling) can be described along the lines of a single-user waveform estimator in [27] as follows

$$\hat{h}_k(t) = \frac{1}{N_p}\sum_{m'=1}^{N_p} A_{k,m'}r_{m'}(t). \tag{8}$$

The estimator requires delay elements, multipliers, and adders.

Detection of either PAM or PPM symbol continued employing the estimated waveform. Consider detection of the n-th symbol $I_{k,n}$ of user k. Correspondingly, there are N_f segments $r_m(t)$ for $m = nN_f, \cdots, (n+1)N_f - 1$. If we assume all $A_{k,m}$ are known to the receiver such as in the uplink, then contribution of reference signals $A_{k,m}h_k(t)$ from all users can be subtracted from $r_m(t)$ after waveforms from all users are estimated. This subtraction process is essential when reference and data pulses overlap after channel distortion, but unnecessary in the conventional TR scheme because of a restrictive assumption of no overlapping (large enough spacing between two pulses that sacrifices data rate). In a case when only the desired users PN sequence $A_{k,m}$ is known, such as in a downlink, only the desired user's reference signal is subtracted. Denote the generic signal after subtraction by $\tilde{r}_{k,m}(t)$. This signal contains the signal part $B_{k,m}I_{k,n}h_k(t - c_{k,m}T_c)$ and interference plus noise part according to our PAM data model. Then, assisted by time hopping code $c_{k,m}$ and the other user specific PN sequence $B_{k,m}$ modulating its data pulse, we can obtain the following signal that carries its data

$$\bar{r}_{k,m}(t) \triangleq B_{k,m}\tilde{r}_{k,m}(t + c_{k,m}T_c). \tag{9}$$

Afterwards, PAM modulated input $I_{k,n}$ can be estimated based on outputs of N_f correlators in the n-th symbol interval via

$$\hat{I}_{k,n} = sign\Big(\frac{1}{N_f}\sum_{m=nN_f}^{(n+1)N_f-1}\int_0^{T_f}\hat{h}_k(t)\bar{r}_{k,m}(t)dt\Big). \tag{10}$$

A simplified receiver block diagram is shown in figure 2, where a reference signal subtraction sub-block is omitted for clearer presentation.

Various summations are required, and upper and lower limits for corresponding indices need to be clearly stated. For notational convenience, we will hereafter omit limits but follow the same convention for time indices m' and m, given by m' from 1 to N_p and m from nN_f to $(n+1)N_f - 1$. Others include user index l (possibly additional ones as l_1, l_2) from 1 to K, and modulation index i (possibly additional ones as i_1, i_2) from 0 to 1.

For the PPM modulated input, a template from the estimated waveform is constructed as $\hat{h}_k(t) - \hat{h}_k(t - \alpha T_c)$, which replaces $\hat{h}_k(t)$ in (10), and also a simple mapping from $\{\pm 1\}$ to $\{0, 1\}$ is performed. Then, the detection criterion for a PPM symbol becomes [7]

$$\hat{I}_{k,n} = \frac{1}{2}(1 - y_{k,n}), \tag{11}$$

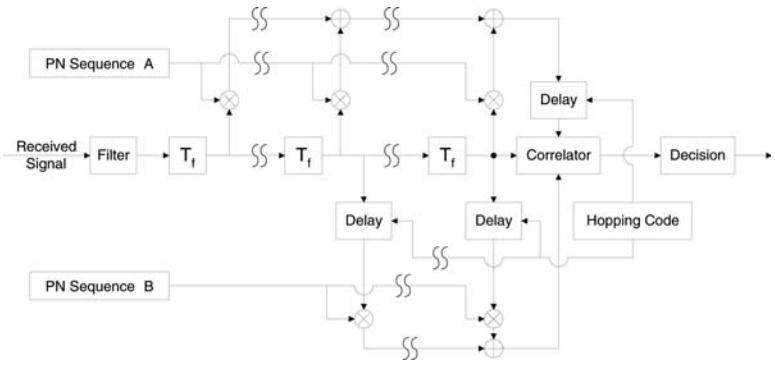

Figure 2: Block diagram of an MTR-UWB receiver.

where $y_{k,n}$ is the detector's output taking $\{\pm 1\}$

$$y_{k,n} = sign\Big(\frac{1}{N_f}\sum_{m}\int_0^{T_f}[\hat{h}_k(t) - \hat{h}_k(t-\alpha T_c)]\bar{r}_{k,m}(t)dt\Big). \tag{12}$$

A receiver block diagram similar to figure 2 can be obtained. In the next section we jointly analyze PAM and PPM detector performance with waveform estimate given by (8).

4 Performance of Waveform Estimators and Detectors

Given N_p received signal segments, our waveform estimator depends on the received signal statistics. Subsequently, the detector performance is also dependent on these statistics. To quantify the waveform estimation performance, define a waveform estimation error $\delta h_k(t) = \hat{h}_k(t) - h_k(t)$ for user k, and the corresponding MSE as

$$MSE_k = \int_0^{T_f} E\Big\{[\delta h_k(t)]^2\Big\}dt, \tag{13}$$

where T_f is the maximum channel delay spread. If it is beyond T_f, then the upper limit of the integral needs to be increased together with duration of each segment $r_{m'}(t)$ used for waveform estimation. The BER of each detector with imperfect template will be evaluated. For tractable analysis, we approximate binary PN sequences as random sequences with zero mean and unit variance. This assumption can yield reliable results for a large sample size, as demonstrated in an aperiodic CDMA system [34]. Next we focus on the PAM case, followed by PPM.

4.1 PAM Signaling

MSE evaluation requires $E\{[\delta h_k(t)]^2\}$. Our derivation starts from waveform estimation error $\delta h_k(t)$ based on the estimator and received data model. Substituting (4) in (8), $\delta h_k(t)$ can be expressed as

$$\begin{aligned}\delta h_k(t) &= \frac{1}{N_p}\sum_{m'}\sum_{l,l\neq k} A_{k,m'}A_{l,m'}h_l(t) + \frac{1}{N_p}\sum_{m'} A_{k,m'}v_{m'}(t) \\ &+ \frac{1}{N_p}\sum_{l,m'} A_{k,m'}B_{l,m'}I_{l,\lfloor m'/N_f\rfloor}h_l(t-c_{l,m'}T_c). \end{aligned} \tag{14}$$

It consists of noise, reference signals, and data signals. For easy later derivation of BER, consider a general term $E\{\delta h_k(t+a)\delta h_k(\tau+b)\}$, which encompasses the special case required in (13) by setting $a=b=0$ and $t=\tau$.

The noise statistics are first derived. For ideal bandpass filter $g(t)$ with unit frequency response over $f\in[-\frac{\mathcal{B}}{2},\frac{\mathcal{B}}{2}]$, then

$$g(t) = \frac{\sin(\pi\mathcal{B}t)}{\pi t} = \mathcal{B}\ \mathrm{sinc}(\pi\mathcal{B}t).$$

Noticing $v(t) = n(t)\star g(t)$ and $E\{n(t)n(\tau)\} = \frac{N_0}{2}\delta(t-\tau)$, the autocorrelation of $v(t)$ and $v(\tau)$ becomes

$$E\{v(t)v(\tau)\} = \frac{N_0}{2}\int_{-\infty}^{\infty} g(t-x)g(\tau-x)dx = \frac{N_0}{2}g(t)\star g(\tau-t).$$

Since the Fourier transform of $g(\tau-t)$ is $e^{-j2\pi f\tau}$ for $f\in[-\frac{\mathcal{B}}{2},\frac{\mathcal{B}}{2}]$, we obtain

$$E\{v(t)v(\tau)\} = \frac{N_0}{2}\int_{-\frac{\mathcal{B}}{2}}^{\frac{\mathcal{B}}{2}} e^{j2\pi f(t-\tau)}df = \sigma_v^2\phi(t-\tau), \quad \sigma_v^2\triangleq\frac{N_0}{2}\mathcal{B}, \quad \phi(t)\triangleq\mathrm{sinc}(\pi\mathcal{B}t).$$

According to (14) and invoking assumptions on PN codes, inputs and noise, we obtain statistics of the waveform estimation error

$$\begin{aligned}E\{\delta h_k(t+a)\delta h_k(\tau+b)\} &= \frac{1}{N_p}\sum_{l,l\neq k} h_l(t+a)h_l(\tau+b) + \frac{\sigma_v^2}{N_p}\phi(t+a-\tau-b) \\ &+ \frac{1}{N_p^2}\sum_{l,m'} h_l(t+a-c_{l,m'}T_c)h_l(\tau+b-c_{l,m'}T_c). \end{aligned} \tag{15}$$

To evaluate MSE in (13), define a deterministic cross correlation of PAM templates of users l_1 and l_2 at offsets d_1T_c and d_2T_c as

$$\mathcal{E}_{l_1,l_2,d_1,d_2} \triangleq \int_0^{T_f} h_{l_1}(t-d_1T_c)h_{l_2}(t-d_2T_c)dt,$$

For convenience in subsequent discussions, similarly define a cross correlation of a waveform at offset d_1T_c and a PPM template at offset d_2T_c as

$$\mathcal{F}_{l_1,l_2,d_1,d_2} \triangleq \int_0^{T_f} h_{l_1}(t-d_1T_c)\Psi_{l_2,d_2}(t)dt, \quad \Psi_{k,d}(t) \triangleq h_k(t-dT_c) - h_k(t-dT_c-\alpha T_c).$$

and define

$$\mathcal{H}_{k,d} \triangleq \iint_0^{T_f} \phi(t-\tau)h_k(t-dT_c)h_k(\tau-dT_c)dt\,d\tau, \quad \mathcal{Q}_{k,d} \triangleq \iint_0^{T_f} \phi(t-\tau)\Psi_{k,d}(t)\Psi_{k,d}(\tau)dt\,d\tau,$$

$$\mathcal{R}_{k,d} \triangleq \iint_0^{T_f} \Big[2\phi(t-\tau) - \phi(t-\tau+\alpha T_c) - \phi(t-\tau-\alpha T_c)\Big]h_k(t-dT_c)h_k(\tau-dT_c)dt\,d\tau,$$

$$\mathcal{X} \triangleq \iint_0^{T_f} \phi(t-\tau)\Big[2\phi(t-\tau) - \phi(t-\tau+\alpha T_c) - \phi(t-\tau-\alpha T_c)\Big]dt\,d\tau, \quad \mathcal{Y} \triangleq \iint_0^{T_f} [\phi(t-\tau)]^2 dt\,d\tau.$$

It will become clear that quantities $\mathcal{E}_{l_1,l_2,d_1,d_2}$, $\mathcal{H}_{k,d}$ and $\mathcal{Y}$ are necessary to evaluate performance of PAM based waveform estimators and detectors, while $\mathcal{F}_{l_1,l_2,d_1,d_2}$, $\mathcal{Q}_{k,d}$, $\mathcal{R}_{k,d}$ and $\mathcal{X}$ are needed for the PPM case.

Substituting (15) in (13), and letting $a = b = 0$ and $t = \tau$, the MSE becomes

$$MSE_k = \sum_{l,l\neq k} \frac{\mathcal{E}_{l,l,0,0}}{N_p} + \sum_{l,m'} \frac{\mathcal{E}_{l,l,c_{l,m'},c_{l,m'}}}{N_p^2} + \frac{\sigma_v^2 T_f}{N_p}. \tag{16}$$

If all users use periodic hopping codes with period of T_f, then the frame index m' in $c_{l,m'}$ can be dropped, and $c_{l,m'}$ is denoted as c_l. Then (16) becomes

$$MSE_k = \sum_{l,l\neq k} \frac{\mathcal{E}_{l,l,0,0}}{N_p} + \sum_{l} \frac{\mathcal{E}_{l,l,c_l,c_l}}{N_p} + \frac{\sigma_v^2 T_f}{N_p}. \tag{17}$$

The first summation has autocorrelations of interfering users waveforms without offset; the second summation contains autocorrelations of all users' waveforms at offsets equal to delays of their data pulses (determined by hopping codes); the last term results from noise. The MSE is inversely proportional to the sample size (number of frame segments N_p). If only one segment from one symbol interval is used in the estimator, then the MSE level may be unacceptable and the template too noisy. That is the case of the conventional

detector. If N_f segments from one symbol interval ($N_s = 1$) are used, then MSE decreases [20], [25]. Our windowed smoothing of received signals across multiple symbol intervals significantly reduces waveform estimation error and improves detection quality. The degree of improvement depends on the window size. Also observe that, if $K = 1$ and $N_f = 1$, then it conforms to the result for a single-user system [27]. But when $N_f > 1$, introducing PN sequence $B_{k,n}$ to the data pulse helps to lower the MSE by a factor of N_f (embedded in N_p) compared to the scheme in [27] without PN sequence covering.

Based upon the above result, analysis of the PAM-based detector can be continued. There are two cases in detection. One corresponds to downlink where only the desired user's PN sequences and hopping codes are known. The other is for uplink communication where all users' PN sequences and hopping codes are available.

4.1.1 UWB downlink

The desired user's waveform is estimated first, based on its PN sequence $A_{k,m'}$. Then, given its PN sequence $A_{k,m}$, its reference signals are subtracted to obtain N_f segments $\tilde{r}_{k,m}(t)$ in the n-th symbol interval. Afterwards, N_f generic signals $(m = nN_f, \cdots, nN_f + N_f - 1)$ are given by

$$\tilde{r}_{k,m}(t) = I_{k,n}B_{k,m}h_k(t - c_{k,m}T_c) - A_{k,m}\delta h_k(t) + \sum_{l,l\neq k}[A_{l,m}h_l(t) + I_{l,n}B_{l,m}h_l(t - c_{l,m}T_c)] + v_m(t), \tag{18}$$

and subsequently (9) becomes

$$\bar{r}_{k,m}(t) = I_{k,n}h_k(t) + u_{k,m}(t) \tag{19}$$

where $u_{k,m}(t)$ represents waveform estimation error, MAI, plus noise,

$$\begin{aligned} nu_{k,m}(t) &= -A_{k,m}B_{k,m}\delta h_k(t + c_{k,m}T_c) + B_{k,m}v_m(t + c_{k,m}T_c) \\ &+ \sum_{l,l\neq k}[A_{l,m}B_{k,m}h_l(t + c_{k,m}T_c) + B_{l,m}B_{k,m}I_{l,n}h_l(t + c_{k,m}T_c - c_{l,m}T_c)]. \end{aligned} \tag{20}$$

Expressing the estimated template as $h_k(t) + \delta h_k(t)$, and substituting (19) into the detector (10), signal and noise components can be identified as

$$z_s = I_{k,n}\mathcal{E}_{k,k,0,0}, \tag{21}$$

$$z_n = I_{k,n}\int_0^{T_f}\delta h_k(t)h_k(t)dt + \frac{1}{N_f}\sum_m\int_0^{T_f}h_k(t)u_{k,m}(t)dt + \frac{1}{N_f}\sum_m\int_0^{T_f}\delta h_k(t)u_{k,m}(t)dt. \tag{22}$$

Assume z_n is a Gaussian random variable. According to the central limit theorem, this assumption is reasonable when N_p is large since $\delta h_k(t)$ given by (14) stems from the sum of many terms, and it directly contributes to both $u_{k,m}(t)$ and z_n. Then the BER of the detector depends on the signal to noise ratio. The signal power is easily found to be $\epsilon_s = \mathcal{E}^2_{k,k,0,0}$. To evaluate the power of z_n, statistics of $\delta h_k(t)$ and $u_{k,m}(t)$ are required. If those N_p segments used for waveform estimation exclude N_f segments in the current (n-th) symbol interval, clearly all terms in the expression of $u_{k,m}(t)$ in (20), except the first, are independent of $\delta h_k(t)$. Even if those N_f segments are used, it is still plausible to assume that they are independent of $\delta h_k(t)$ for simplified expressions, since the waveform may be typically estimated based on $N_p \gg N_f$ segments. Under this assumption, we obtain the power $\epsilon_n = E\{z_n^2\}$ as

$$\begin{aligned} n\epsilon_n &= \iint_0^{T_f} E\{\delta h_k(t)\delta h_k(\tau)\}h_k(t)h_k(\tau)dt\,d\tau \\ &+ \frac{1}{N_f^2}\sum_m \iint_0^{T_f} h_k(t)h_k(\tau)E\{u_{k,m}(t)u_{k,m}(\tau)\}dt\,d\tau \\ &+ \frac{1}{N_f^2}\sum_m \iint_0^{T_f} E\{\delta h_k(t)\delta h_k(\tau)\}E\{u_{k,m}(t)u_{k,m}(\tau)\}dt\,d\tau. \end{aligned} \tag{23}$$

Although statistics of $\delta h_k(t)$ have been derived, simplification of ϵ_n requires statistics of $u_{k,m}(t)$. From (20), we find

$$\begin{aligned} E\{u_{k,m}(t)u_{k,m}(\tau)\} &= E\{\delta h_k(t+c_{k,m}T_c)\delta h_k(\tau+c_{k,m}T_c)\} + \sigma_v^2\phi(t-\tau) \\ &+ \sum_{l,l\neq k} h_l(t+c_{k,m}T_c)h_l(\tau+c_{k,m}T_c) \\ &+ \sum_{l,l\neq k} h_l(t+c_{k,m}T_c-c_{l,m}T_c)h_l(\tau+c_{k,m}T_c-c_{l,m}T_c). \end{aligned} \tag{24}$$

Applying (15), this becomes

$$\begin{aligned} E\{u_{k,m}(t)u_{k,m}(\tau)\} &= \frac{1}{N_p}\sum_{l,l\neq k} h_l(t+c_{k,m}T_c)h_l(\tau+c_{k,m}T_c) + (1+\frac{1}{N_p})\sigma_v^2\phi(t-\tau) \\ &+ \frac{1}{N_p^2}\sum_{l,m'} h_l(t+c_{k,m}T_c-c_{l,m'}T_c)h_l(\tau+c_{k,m}T_c-c_{l,m'}T_c) \\ &+ \sum_{l,l\neq k} h_l(t+c_{k,m}T_c)h_l(\tau+c_{k,m}T_c) \\ &+ \sum_{l,l\neq k} h_l(t+c_{k,m}T_c-c_{l,m}T_c)h_l(\tau+c_{k,m}T_c-c_{l,m}T_c). \end{aligned} \tag{25}$$

Substituting (25) and (15) into (23), the interference plus noise power is

$$\begin{aligned}
\epsilon_n &= \sum_{l,l\neq k}\frac{\mathcal{E}^2_{k,l,0,0}}{N_p}+(\frac{\sigma_v^2}{N_f}+\frac{\sigma_v^2}{N_p}+\frac{\sigma_v^2}{N_fN_p})\mathcal{H}_{k,0}+\sum_{l,m'}\frac{\mathcal{E}^2_{k,l,0,c_{l,m'}}}{N_p^2}\\
&+ \sum_m\sum_{l,l\neq k}\frac{\mathcal{E}^2_{k,l,0,-c_{k,m}}}{N_f^2N_p}+\sum_{l,m,m'}\frac{\mathcal{E}^2_{k,l,0,c_{l,m'}-c_{k,m}}}{N_f^2N_p^2}+\sum_m\sum_{l,l\neq k}\frac{\mathcal{E}^2_{k,l,0,-c_{k,m}}}{N_f^2}+\sum_m\sum_{l,l\neq k}\frac{\mathcal{E}^2_{k,l,0,c_{l,m}-c_{k,m}}}{N_f^2}\\
&+ \sum_{l,l\neq k}\frac{\sigma_v^2}{N_fN_p}\mathcal{H}_{l,0}+\frac{\sigma_v^4}{N_fN_p}\mathcal{Y}+\sum_{l,m'}\frac{\sigma_v^2}{N_fN_p^2}\mathcal{H}_{l,c_{l,m'}}\\
&+ \sum_m\sum_{l_1,l_2,l_1\neq k,l_2\neq k}(\frac{\mathcal{E}^2_{l_1,l_2,0,-c_{k,m}}}{N_f^2N_p}+\frac{\mathcal{E}^2_{l_1,l_2,0,c_{l_2,m}-c_{k,m}}}{N_f^2N_p})\\
&+ \sum_m\sum_{l,l\neq k}(\frac{\sigma_v^2}{N_f^2N_p}\mathcal{H}_{l,-c_{k,m}}+\frac{\sigma_v^2}{N_f^2N_p}\mathcal{H}_{l,c_{l,m}-c_{k,m}})\\
&+ \sum_{l_1,m,m'}\sum_{l_2,l_2\neq k}(\frac{\mathcal{E}^2_{l_1,l_2,c_{l_1,m'},-c_{k,m}}}{N_f^2N_p^2}+\frac{\mathcal{E}^2_{l_1,l_2,c_{l_1,m'},c_{l_2,m}-c_{k,m}}}{N_f^2N_p^2}),
\end{aligned}\tag{26}$$

where all terms of order $\frac{1}{N_p^2}$ in simplifying the third term of (23) have been ignored. However, terms with $\frac{1}{N_p^2}\sum_{m'}$ are kept since they are of order $\frac{1}{N_p}$ due to summation of m' from 1 to N_p. If each hopping sequence is assumed periodic to reduce implementation cost, then this reduces to

$$\begin{aligned}
\epsilon_n &= (\frac{\sigma_v^2}{N_f}+\frac{\sigma_v^2}{N_p}+\frac{\sigma_v^2}{N_fN_p})\mathcal{H}_{k,0}+\frac{\sigma_v^4}{N_fN_p}\mathcal{Y}+\sum_l(\frac{\mathcal{E}^2_{k,l,0,c_l}}{N_p}+\frac{\mathcal{E}^2_{k,l,0,c_l-c_k}}{N_fN_p}+\frac{\sigma_v^2\mathcal{H}_{l,c_l}}{N_fN_p})\\
&+ \sum_{l,l\neq k}\big[(\frac{1}{N_f}+\frac{1}{N_fN_p})\mathcal{E}^2_{k,l,0,-c_k}+\frac{\mathcal{E}^2_{k,l,0,c_l-c_k}}{N_f}+\frac{\mathcal{E}^2_{k,l,0,0}}{N_p}+\frac{\sigma_v^2\mathcal{H}_{l,0}}{N_fN_p}+\frac{\sigma_v^2\mathcal{H}_{l,-c_k}}{N_fN_p}+\frac{\sigma_v^2\mathcal{H}_{l,c_l-c_k}}{N_fN_p}\big]\\
&+ \sum_{l_1,l_2,l_1\neq k,l_2\neq k}(\frac{\mathcal{E}^2_{l_1,l_2,0,-c_k}}{N_fN_p}+\frac{\mathcal{E}^2_{l_1,l_2,0,c_{l_2}-c_k}}{N_fN_p})+\sum_{l_1}\sum_{l_2,l_2\neq k}(\frac{\mathcal{E}^2_{l_1,l_2,c_{l_1},-c_k}}{N_fN_p}+\frac{\mathcal{E}^2_{l_1,l_2,c_{l_1},c_{l_2}-c_k}}{N_fN_p}).
\end{aligned}\tag{27}$$

Once again, the power is observed to depend on autocorrelations as well as cross correlations $\mathcal{E}_{l_1,l_2,d_1,d_2}$ of all users waveforms with different offsets, where offsets depend on the hopping codes. Clearly, the larger difference in codes, the smaller their correlations. Thus introduction of different hopping codes helps to reduce interference power since hopping codes alleviate terms at a typical offset $(c_l-c_k)T_c$ in (27), such as the second to the last term in the first line, as well as two terms in the second and third lines, respectively. It is expected that if asynchrony is considered in the received data model to characterize different time of arrivals, then ϵ_n will be further decreased based on the same

reasoning. Noise contributions are reflected by terms $\mathcal{H}_{k,d}$ and $\mathcal{Y}$. Most terms in (27) are inversely proportional to sample size N_p, so increasing N_p will decrease ϵ_n as well. However, there is a lower bound dominated by those terms dependent only on N_f, which corresponds to the limiting case $N_p \to \infty$. The result in this case is given by

$$\epsilon_n = \frac{\sigma_v^2}{N_f}\mathcal{H}_{k,0} + \sum_{l,l\neq k}(\frac{\mathcal{E}^2_{k,l,0,-c_k}}{N_f} + \frac{\mathcal{E}^2_{k,l,0,c_l-c_k}}{N_f}). \tag{28}$$

This means that even in the absence of waveform estimation error ($MSE_k \to 0$ as $N_p \to \infty$ according to (17)), interference from other users data pulses plus noise in those N_f segments of the n-th symbol interval are non-trivial. In this case, ϵ_n is inversely proportional to N_f. So, increasing N_f is desirable while meeting the data rate requirement. Similar observations can be made for other communication scenarios described below.

The BER of the detector depends on the signal to interference plus noise ratio. As discussed before, the interference plus noise can be well modeled as a Gaussian process. Then, given signal power ϵ_s and interference plus noise power ϵ_n, the BER of our detector can be evaluated as $Q(\sqrt{\frac{\epsilon_s}{\epsilon_n}})$ where $Q(x)$ is a Q-function given by $Q(x) = \int_x^\infty \frac{1}{\sqrt{2\pi}} e^{-\frac{x^2}{2}} dx$. Similarly, we will later derive signal power and interference pulse noise power for other cases. Due to some similarities, derivations will be briefed only.

4.1.2 UWB uplink

In this case, each user's waveform can be estimated by (8) based on PN sequence $A_{k,m'}$. Then the estimated reference signal $A_{k,m}\hat{h}_k(t)$ is subtracted, yielding the following signal

$$\tilde{r}_{k,m}(t) = I_{k,n}B_{k,m}h_k(t-c_{k,m}T_c) - A_{k,m}\delta h_k(t) - \sum_{l,l\neq k} A_{l,m}\delta h_l(t) + \sum_{l,l\neq k} I_{l,n}B_{l,m}h_l(t-c_{l,m}T_c) + v_m(t). \tag{29}$$

Now

$$\bar{r}_{k,m}(t) = I_{k,n}h_k(t) + u_{k,m}(t), \tag{30}$$

where $u_{k,m}(t)$ is given by

$$\begin{aligned} u_{k,m}(t) &= -\sum_l A_{l,m}B_{k,m}\delta h_l(t + c_{k,m}T_c) + B_{k,m}v_m(t + c_{k,m}T_c) \\ &+ \sum_{l,l\neq k} B_{l,m}B_{k,m}I_{l,n}h_l(t + c_{k,m}T_c - c_{l,m}T_c). \end{aligned} \tag{31}$$

For the detector (10), signal z_s, interference and noise z_n still follow (21) and (22), and $\epsilon_s = \mathcal{E}^2_{k,k,0,0}$. However, $u_{k,m}(t)$ in (31) is different from (20), so ϵ_n needs to be re-derived. It is shown in Appendix subsection A.1 that if all time hopping sequences are periodic, then

$$\begin{aligned}
\epsilon_n &= (\frac{\sigma_v^2}{N_f} + \frac{\sigma_v^2}{N_p} + \frac{K\sigma_v^2}{N_f N_p})\mathcal{H}_{k,0} + \frac{\sigma_v^4}{N_f N_p}\mathcal{Y} + \sum_l (\frac{\mathcal{E}^2_{k,l,0,c_l}}{N_p} + \frac{\sigma_v^2 \mathcal{H}_{l,c_l}}{N_f N_p}) \\
&+ \sum_{l,l\neq k} (\frac{\mathcal{E}^2_{k,l,0,c_l-c_k}}{N_f} + \frac{\mathcal{E}^2_{k,l,0,0}}{N_p} + \frac{\sigma_v^2 \mathcal{H}_{l,0}}{N_f N_p} + \frac{\sigma_v^2 \mathcal{H}_{l,c_l-c_k}}{N_f N_p}) + \sum_{l_1,l_2} \frac{\mathcal{E}^2_{k,l_2,0,c_{l_2}-c_{l_1}}}{N_f N_p} \\
&+ \sum_{l_1,l_2,l_1\neq k,l_2\neq k} \frac{\mathcal{E}^2_{l_1,l_2,0,c_{l_2}-c_k}}{N_f N_p} + \sum_{l_1} \sum_{l_2,l_2\neq l_1} \frac{\mathcal{E}^2_{k,l_2,0,-c_{l_1}}}{N_f N_p} + \sum_{l_1} \sum_{l_2,l_2\neq k} \frac{\mathcal{E}^2_{l_1,l_2,c_{l_1},c_{l_2}-c_k}}{N_f N_p}. \quad (32)
\end{aligned}$$

If $N_p \gg 1$, then

$$\epsilon_n = \frac{\sigma_v^2 \mathcal{H}_{k,0}}{N_f} + \sum_{l,l\neq k} \frac{\mathcal{E}^2_{k,l,0,c_l-c_k}}{N_f}. \quad (33)$$

Compared with (28), this power is smaller since reference signals from interfering users are subtracted. This observation also suggests that the first term in the summation of (28) is due to reference signals of interfering users, while the second from their data signals as above.

4.2 PPM Signaling

Substituting (6) into (8), $\delta h_k(t)$ can be expressed as

$$\begin{aligned}
\delta h_k(t) &= \frac{1}{N_p} \sum_{m'} \sum_{l,l\neq k} A_{l,m'} A_{k,m'} h_l(t) + \frac{1}{N_p} \sum_{m'} A_{k,m'} v_{m'}(t) \\
&+ \frac{1}{N_p} \sum_{l,m'} A_{k,m'} B_{l,m'} h_l(t - c_{l,m'} T_c - I_{l,\lfloor m'/N_f \rfloor} \alpha T_c). \quad (34)
\end{aligned}$$

Then invoking our assumptions on PN codes, inputs, and noise, and considering PPM modulation where $I_{l,\lfloor m'/N_f \rfloor}$ takes 0 and 1 with equal probability, we obtain

$$\begin{aligned}
E\{\delta h_k(t+a)\delta h_k(\tau+b)\} &= \frac{1}{N_p} \sum_{l,l\neq k} h_l(t+a) h_l(\tau+b) + \frac{\sigma_v^2}{N_p} \phi(t+a-\tau-b) \\
&+ \frac{1}{2N_p^2} \sum_{i,l,m'} \sum_{i=0}^{1} h_l(t+a-c_{l,m'}T_c - i\alpha T_c) h_l(\tau+b-c_{l,m'}T_c - i\alpha T_c). \quad (35)
\end{aligned}$$

Substituting (35) in (13), and letting $a = b = 0$ and $t = \tau$, the template estimation MSE becomes

$$MSE_k = \sum_{l,l\neq k} \frac{\mathcal{E}_{l,l,0,0}}{N_p} + \sum_{i,l,m'} \frac{\mathcal{E}_{l,l,c_{l,m'}+i\alpha,c_{l,m'}+i\alpha}}{2N_p^2} + \frac{\sigma_v^2 T_f}{N_p}. \tag{36}$$

If all users use periodic hopping sequences, then (36) becomes

$$MSE_k = \sum_{l,l\neq k} \frac{\mathcal{E}_{l,l,0,0}}{N_p} + \sum_{i,l} \frac{\mathcal{E}_{l,l,c_l+i\alpha,c_l+i\alpha}}{2N_p} + \frac{\sigma_v^2 T_f}{N_p}. \tag{37}$$

Next we consider the two cases for detection of PPM symbols.

4.2.1 UWB downlink

In the n-th symbol interval, N_f generic signals are given by

$$\begin{aligned} \tilde{r}_{k,m}(t) &= B_{k,m} h_k(t - c_{k,m}T_c - \tau_{I_{k,n}}) - A_{k,m}\delta h_k(t) \\ &+ \sum_{l,l\neq k} [A_{l,m} h_l(t) + B_{l,m} h_l(t - c_{l,m}T_c - \tau_{I_{l,n}})] + v_m(t). \end{aligned} \tag{38}$$

Subsequently (9) becomes

$$\bar{r}_{k,m}(t) = h_k(t - I_{k,n}\alpha T_c) + u_{k,m}(t), \tag{39}$$

where modulation delay has been substituted by information controlled shift amount, $u_{k,m}(t)$ represents waveform estimation error, MAI, plus noise, as

$$\begin{aligned} u_{k,m}(t) &= -A_{k,m}B_{k,m}\delta h_k(t + c_{k,m}T_c) + B_{k,m} v_m(t + c_{k,m}T_c) \\ &+ \sum_{l,l\neq k} [A_{l,m}B_{k,m} h_l(t + c_{k,m}T_c) + B_{l,m}B_{k,m} h_l(t + c_{k,m}T_c - c_{l,m}T_c - I_{l,n}\alpha T_c)]. \end{aligned} \tag{40}$$

Expressing estimated waveform (12) used in the detector (11) by $h_k(t) + \delta h_k(t)$, the signal and noise components in $y_{k,m}$ are

$$z_s = \int_0^{T_f} \Psi_{k,0}(t) h_k(t - I_{k,n}\alpha T_c) dt, \tag{41}$$

$$\begin{aligned} z_n &= \int_0^{T_f} \delta\Psi_{k,0}(t) h_k(t - I_{k,n}\alpha T_c) dt + \frac{1}{N_f} \sum_m \int_0^{T_f} \Psi_{k,0}(t) u_{k,m}(t) dt \\ &+ \frac{1}{N_f} \sum_m \int_0^{T_f} \delta\Psi_{k,0}(t) u_{k,m}(t) dt. \end{aligned} \tag{42}$$

The BER of the detector depends on the signal to noise ratio. Given $I_{k,n} = 0$ is transmitted, the signal power is $\epsilon_{0,s} = \mathcal{F}^2_{k,k,0,0}$ while for transmitted $I_{k,n} = 1$, $\epsilon_{1,s} = \mathcal{F}^2_{k,k,\alpha,0}$. It is reasonable to assume the BERs, conditioned on the two different inputs, are approximately the same, a result that we have confirmed with simulation. So we focus on the case when $I_{k,n} = 0$ is transmitted. The signal power is denoted as ϵ_s. The interference and noise power $\epsilon_n = E\{z_n^2\}$, conditioned on $I_{k,n} = 0$, is required to evaluate BER based on the Q-function as $Q(\sqrt{\frac{\epsilon_s}{\epsilon_n}})$. In appendix subsection A.2 it is shown that if each hopping sequence is periodic, then

$$
\begin{aligned}
\epsilon_n &= \frac{\sigma_v^2}{N_p}\mathcal{R}_{k,0} + (\frac{\sigma_v^2}{N_f} + \frac{\sigma_v^2}{N_f N_p})\mathcal{Q}_{k,0} + \frac{\sigma_v^4}{N_f N_p}\mathcal{X} \\
&+ \sum_{l,l\neq k}\Big[\frac{\mathcal{F}^2_{k,l,0,0}}{N_p} + (\frac{1}{N_f} + \frac{1}{N_f N_p})\mathcal{F}^2_{l,k,-c_k,0} + \frac{\sigma_v^2}{N_f N_p}\mathcal{R}_{l,-c_k} + \frac{\sigma_v^2}{N_f N_p}\mathcal{Q}_{l,0}\Big] \\
&+ \sum_{i,l}(\frac{\mathcal{F}^2_{k,l,0,c_l+i\alpha}}{2N_p} + \frac{\mathcal{F}^2_{l,k,c_l-c_k+i\alpha,0}}{2N_f N_p} + \frac{\sigma_v^2}{2N_f N_p}\mathcal{Q}_{l,c_l+i\alpha}) \\
&+ \sum_i\sum_{l,l\neq k}(\frac{\sigma_v^2}{2N_f N_p}\mathcal{R}_{l,c_l-c_k+i\alpha} + \frac{\mathcal{F}^2_{l,k,c_l-c_k+i\alpha,0}}{2N_f}) \\
&+ \sum_{l_1,l_2,l_1\neq k,l_2\neq k}\frac{\mathcal{F}^2_{l_1,l_2,-c_k,0}}{N_f N_p} + \sum_i\sum_{l_1,l_2,l_1\neq k,l_2\neq k}\frac{\mathcal{F}^2_{l_1,l_2,c_{l_1}-c_k+i\alpha,0}}{2N_f N_p} \\
&+ \sum_{i,l_2}\sum_{l_1,l_1\neq k}\frac{\mathcal{F}^2_{l_1,l_2,-c_k,c_{l_2}+i\alpha}}{2N_f N_p} + \sum_{i_1,i_2,l_2}\sum_{l_1,l_1\neq k}\frac{\mathcal{F}^2_{l_1,l_2,c_{l_1}-c_k+i_1\alpha,c_{l_2}+i_2\alpha}}{4N_f N_p}.
\end{aligned}
\tag{43}
$$

Note that $\mathcal{F}_{l_1,l_2,d_1,d_2}$, $\mathcal{Q}_{k,d}$, $\mathcal{R}_{k,d}$ and $\mathcal{X}$ are necessary to evaluate PPM performance. When $N_p \gg 1$, ϵ_n becomes

$$
\epsilon_n = \frac{\sigma_v^2}{N_f}\mathcal{Q}_{k,0} + \sum_{l,l\neq k}\frac{\mathcal{F}^2_{l,k,-c_k,0}}{N_f} + \sum_i\sum_{l,l\neq k}\frac{\mathcal{F}^2_{l,k,c_l-c_k+i\alpha,0}}{2N_f}. \tag{44}
$$

4.2.2 UWB uplink

In this case, each user's waveform can be estimated by (8) and its estimated reference signal $A_{k,m}\hat{h}_k(t)$ is subtracted, yielding the following signal

$$\begin{aligned}\tilde{r}_{k,m}(t) &= B_{k,m}h_k(t-c_{k,m}T_c-\tau_{I_{k,n}})-A_{k,m}\delta h_k(t)-\sum_{l,l\neq k}A_{l,m}\delta h_l(t)\\ &+ \sum_{l,l\neq k}B_{l,m}h_l(t-c_{l,m}T_c-\tau_{I_{l,n}})+v_m(t). \end{aligned} \quad (45)$$

Then

$$\bar{r}_{k,m}(t)=h_k(t-I_{k,n}\alpha T_c)+u_{k,m}(t), \quad (46)$$

with $u_{k,m}(t)$ given by

$$\begin{aligned}u_{k,m}(t) &= -\sum_{l}A_{l,m}B_{k,m}\delta h_l(t+c_{k,m}T_c)+B_{k,m}v_m(t+c_{k,m}T_c)\\ &+ \sum_{l,l\neq k}B_{l,m}B_{k,m}h_l(t+c_{k,m}T_c-c_{l,m}T_c-I_{k,n}\alpha T_c). \end{aligned} \quad (47)$$

For the detector (10), desired signal z_s, interference, and noise z_n have the same forms as (41) and (42), and the signal power is still $\epsilon_{0,s}=\mathcal{F}^2_{k,k,0,0}$. Interference plus noise power is shown in Appendix subsection A.3 to be

$$\begin{aligned}\epsilon_n &= \frac{\sigma_v^2}{N_p}\mathcal{R}_{k,0}+(\frac{\sigma_v^2}{N_f}+\frac{\sigma_v^2K}{N_fN_p})\mathcal{Q}_{k,0}+\frac{\sigma_v^4}{N_fN_p}\mathcal{X}+\sum_{l,l\neq k}(\frac{\mathcal{F}^2_{k,l,0,0}}{N_p}+\frac{\sigma_v^2}{N_fN_p}\mathcal{Q}_{l,0})\\ &+ \sum_{i,l}(\frac{\mathcal{F}^2_{k,l,0,c_l+i\alpha}}{2N_p}+\frac{\sigma_v^2}{2N_fN_p}\mathcal{Q}_{l,c_l+i\alpha})+\sum_i\sum_{l,l\neq k}(\frac{\sigma_v^2}{2N_fN_p}\mathcal{R}_{l,c_l-c_k+i\alpha}+\frac{\mathcal{F}^2_{l,k,c_l-c_k+i\alpha,0}}{2N_f})\\ &+ \sum_{l_1}\sum_{l_2,l_2\neq l_1}\frac{\mathcal{F}^2_{l_2,k,-c_{l_1},0}}{N_fN_p}+\sum_{i,l_1,l_2}\frac{\mathcal{F}^2_{l_2,k,c_{l_2}-c_{l_1}+i\alpha,0}}{2N_fN_p}\\ &+ \sum_i\sum_{l_1,l_2,l_1\neq k,l_2\neq k}\frac{\mathcal{F}^2_{l_1,l_2,c_{l_1}-c_k+i\alpha,0}}{2N_fN_p}+\sum_{i_1,i_2,l_2}\sum_{l_1,l_1\neq k}\frac{\mathcal{F}^2_{l_1,l_2,c_{l_1}-c_k+i_1\alpha,c_{l_2}+i_2\alpha}}{4N_fN_p} \end{aligned} \quad (48)$$

when each hopping sequence is periodic. In a case of $N_p\gg 1$, it becomes

$$\epsilon_n=\frac{\sigma_v^2}{N_f}\mathcal{Q}_{k,0}+\sum_i\sum_{l,l\neq k}\frac{\mathcal{F}^2_{l,k,c_l-c_k+i\alpha,0}}{2N_f} \quad (49)$$

which is smaller than (44).

4.3 Brief Summary

Although some observations have been made before, it is helpful to compare different detectors. For each data modulation, the uplink detector outperforms the downlink detector. For example, compare (27) or (28) with (32) or (33) with PAM signaling; compare (43) or (44) with (48) or (49) with PPM signaling. However, the uplink detector does not attempt to detect inputs from all users simultaneously even though all users' signal waveforms can be estimated concurrently. Rather, each detector estimates user input one at a time. The estimated data signals from other users can be successively cancelled, similar to cancellation of reference signals. Although perhaps not obvious, the superiority of PAM over PPM signaling, in terms of estimation and detection performance, has been observed for a single-user system without PN coding [27], and will also be supported by simulation results presented next.

5 Numerical Examples

The proposed waveform estimators and detectors are tested, and their corresponding analytical results are verified by computer simulation. Both MSE, normalized by the autocorrelation of the waveform at zero offset, and detection BER are presented. The second derivative of Gaussian pulse $w(t) = \Big[1 - 4\pi(\frac{t-D_g/2}{\tau_m})^2\Big] exp\Big[-2\pi(\frac{t-D_g/2}{\tau_m})^2\Big]$ is adopted as the transmitted pulse with $D_g = 0.7ns$ and $\tau_m = 0.2877ns$ [7]. For the PPM based UWB system, modulation delay is $\sigma_d = 0.156ns$ [7]. Except when stated otherwise, the following typical parameters are set: $N_s = 500$, $N_f = 2$, $T_c = 1ns$, $K = 4$, $E_b/N_0 = 10B$, $D = 3$, $D_{max} = D + K$. Binary PN sequences are generated randomly. Each user's TH code is chosen randomly from a set $\{D, \cdots, D_{max}\}$ in each of 100 independent channel realizations where channels are generated according to the IEEE UWB CM1 channel model [33]. To avoid unnecessary calculations, only multipath components are used to ensure 99% total energy capture, while many small trailing coefficients are ignored. The bandwidth of the front-end bandpass filter is chosen to be twice the higher 3 dB cut-off frequency of the monopulse. T_f is set to be slightly larger than the maximum channel delay spread, on the order of tens of nanoseconds, because of long channel tails. Considering a relatively small D and large channel delay spread, severe IPI at the receiver occurs. Effects of sample size N_s, noise in terms of E_b/N_0, number of users, near-far interference, and channel conditions (using the IEEE channel models CM1 to CM4) are studied. For each scenario, both PAM and PPM results are shown, including uplink and downlink cases.

5.1 Effect of Sample Size

The MSE is predicted to be inversely proportional to sample size and the BER is lower bounded the when sample size is sufficiently large. Figure 3 shows MSE versus sample size for PAM signaling. Results marked by "*" are based on experiment, while the solid line is from analysis. Clearly, analytical results are consistent with those from experiments. The MSE level is favorably low. For example, it is below 1×10^{-1} with 500 symbols transmitted. (We have compared MSE analysis and simulation for our other cases and observed an exact match, and so only BER results will be shown hereafter.) BER performance is demonstrated in figure 4. Curves with upward point triangles are for uplink, and those with downward triangles are for downlink, with stars for the conventional receiver. Solid lines are experimental results. Dashed lines represent bounds, where the true noise-free waveforms are used in the detector. Dashed-dotted lines are based on analysis. Experimental results converge to both analytical ones and bounds as the sample size increases to about 1000. The uplink detector is better than the downlink one for a large sample size. Both detectors significantly outperform the conventional one that uses a very noisy template.

For PPM signaling, BER results are plotted in figure 5. Similar conclusions can be made. Comparing to PAM signaling, BER convergence of experimental results to both analytical results and bounds appear faster as early as 500 samples. But the BERs are larger. For both PAM and PPM modulation formats, the raw BERs can achieve 3×10^{-2} with only 50 samples used for waveform estimation.

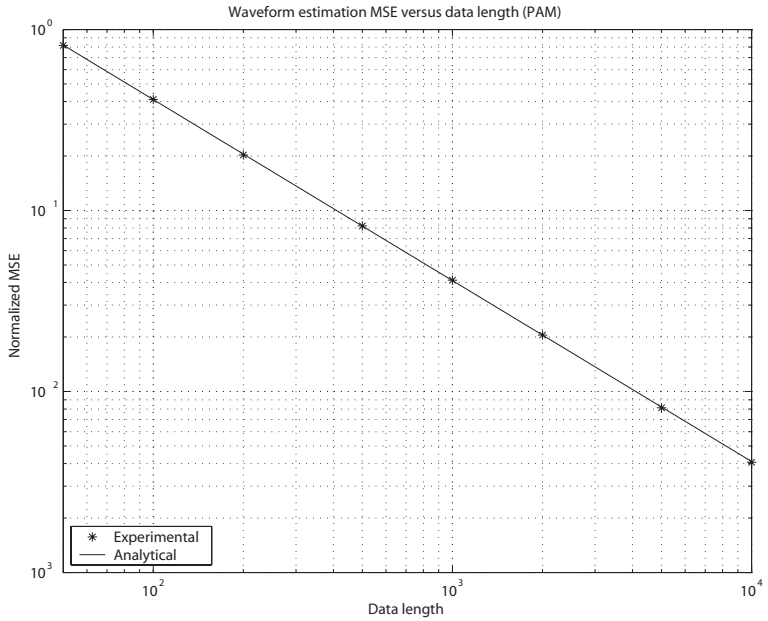

Figure 3: Normalized waveform estimation MSE versus data length with PAM signaling.

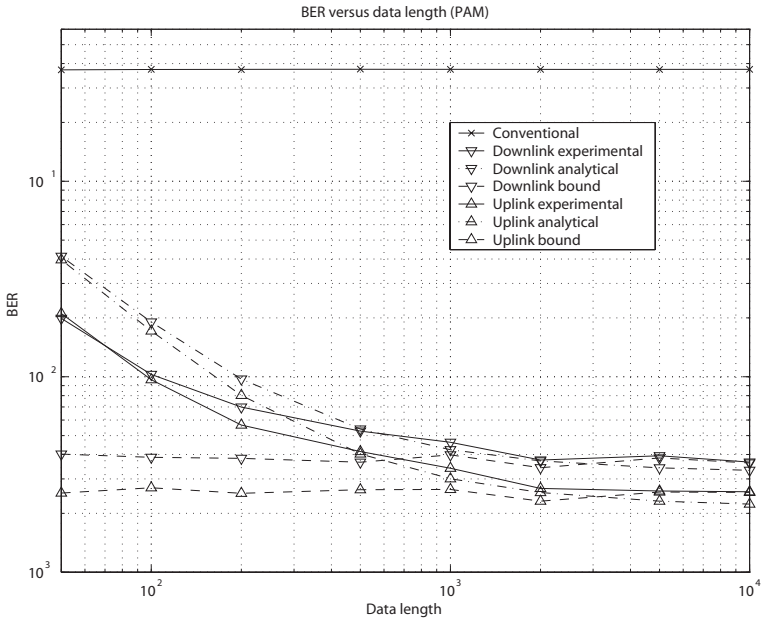

Figure 4: BER versus data length with PAM signaling.

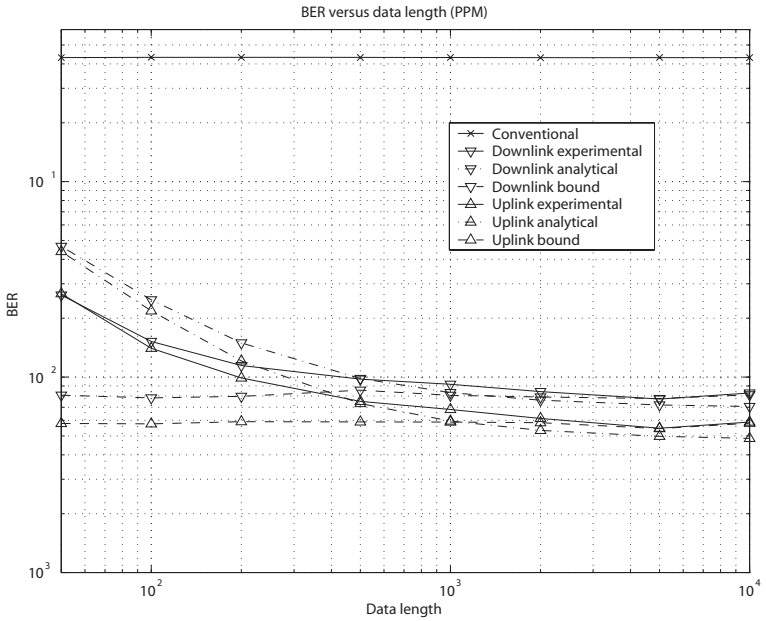

Figure 5: BER versus data length with PPM signaling.

5.2 Effect of Noise

Noise is another factor that significantly affects detection performance. Figure 6 shows its effect on the BER with PAM signaling. The signal to noise ratio E_b/N_0 ranges from 0 dB to 12 dB. Reliable detection is seen from figure 6, and the proposed detectors substantially outperform the conventional TR scheme. Uplink detector is better than downlink detector at high SNR. For each proposed detector, analytical curves agree well with experimental ones. Again, small gaps from associated bounds are due to the finite sample effect on the proposed detectors, as already observed from the result of figure 4, e.g., at the point 500 samples with $E_b/N_0 = 10$ dB. Corresponding BERs for PPM signaling are presented figure 7. Comparing with PAM results, the BERs are slightly larger than those with PAM, and gaps between experimental and analytical results are smaller. This is consistent with observed faster convergence with respect to sample size indicated by figure 5.

Due to excellent convergence of analytical and experimental results observed in the above cases, we will rely on the analytical results hereafter to study receiver performance when the number of users, interference power, and channel conditions vary.

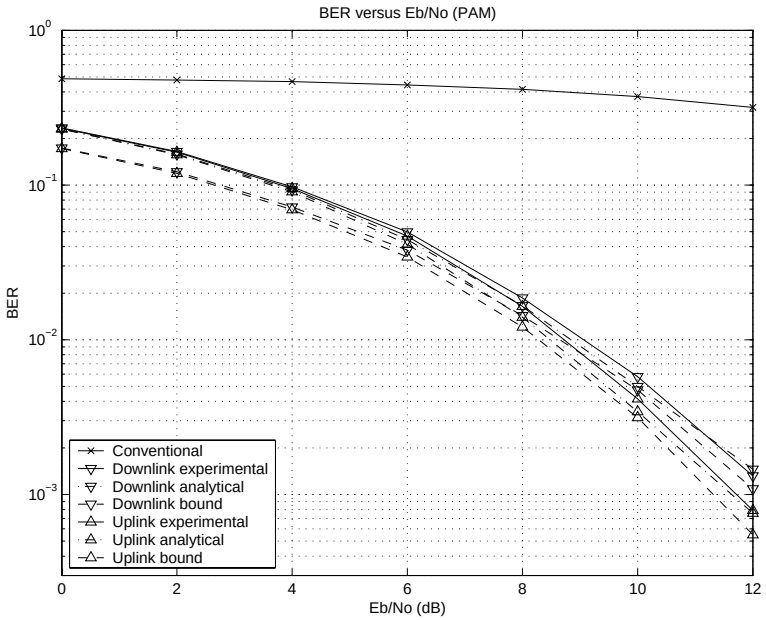

Figure 6: BER versus Eb/No with PAM signaling.

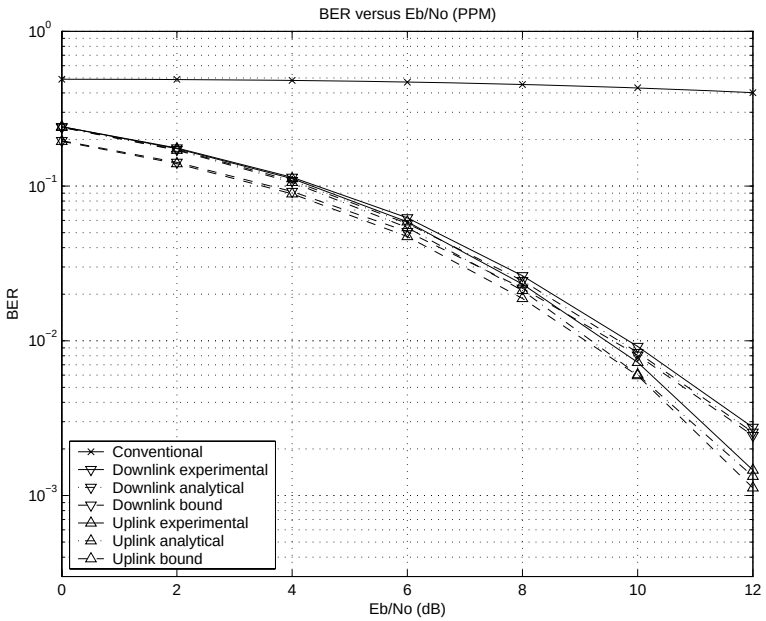

Figure 7: BER versus Eb/No with PPM signaling.

5.3 Effect of Number of Users

It is desirable for a UWB system to maximize its capacity. However, the number of users in the system controls the interference level to the desired user. Based on our analytical results, figure 8 demonstrates the MAI effect on BER of downlink and uplink detectors for both PAM and PPM. Again, 100 independent channel realizations are conducted under $E_b/N_0 = 10\ dB$, and $N_s = 500$. K varies from 1 up to 36, but D_{max} is fixed at 8 to make a fair comparison. Solid lines are for PAM signaling and dashed lines for PPM signaling. Each detector degrades with increasing K, and all detectors are able to provide raw BERs as low as 1×10^{-2} with 5 users. Uplink detector with PAM signaling performs the best, while downlink detector with PPM signaling the worst. Downlink detector with PAM signaling performs better than uplink detector with PPM signaling when there are fewer than 8 users, with the conclusion reversed with many users. Overall, PAM signaling is advantageous to PPM signaling, and the performance difference between an uplink and downlink detector increases as K increases.

5.4 Near-far Effect

Next we consider a near-far scenario, with results shown in figure 9. Define the signal to interference ratio (SIR) as the ratio of the desired user's transmitted power to each of equally powered interfering users in a 4-user system with $10dB$ noise. SIR ranges from

$-20dB$ to $20dB$. If it is desirable to achieve BER about 1×10^{-2}, then $-5dB$ SIR can be tolerated. Convergence levels coincide with the single user bounds for each modulation, shown by starting points in figure 8.

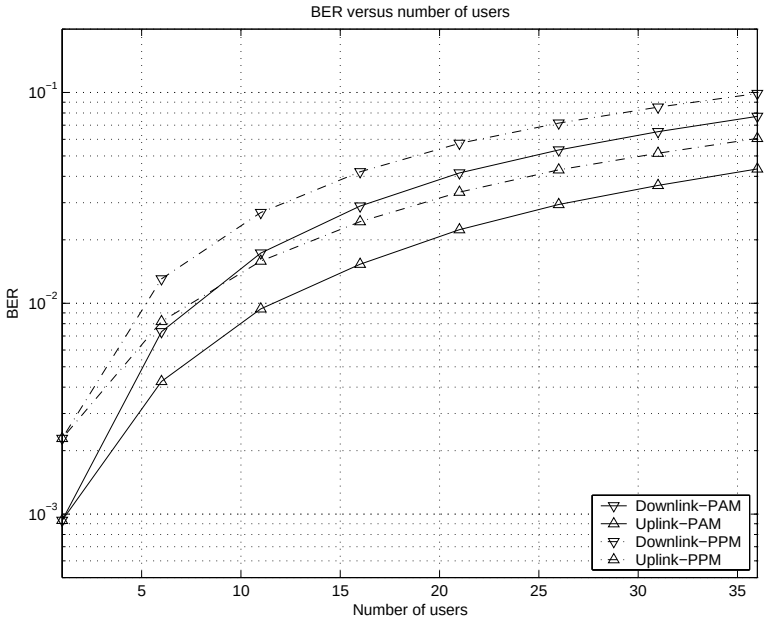

Figure 8: Effect of number of users on BER.

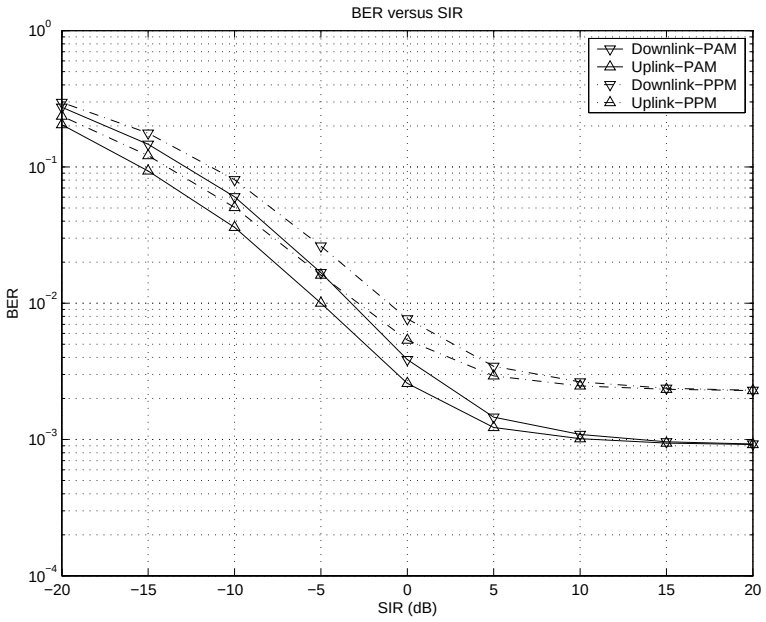

Figure 9: Near-far effect on desired user BER.

5.5 Effect of Channel Characteristics

IEEE UWB channel model CM1 to generate independent channels. Currently, four UWB channel models are available from the IEEE, namely CM1 to CM4 [26]. They capture typical link characteristics for short to medium range, line of sight (LOS) or non-line of sight (NLOS) communications. CM1 is for LOS at range 0-4m, CM2 is for NLOS at the same range, CM3 is for NLOS at 4-10m, CM4 is to fit a $25ns$ root mean square delay spread to represent an extreme NLOS multipath channel. All those models are considered to generate different channel characteristics. Their effects on analytical BERs are investigated. In order for manageable realization of detectors in a computer, multipath channels generated by CM4 are truncated at the point of 80% total energy capture. Figure 10 shows results under a similar setup as described above. Interestingly, all four detectors favor CM4. Rich scattering is not an adverse factor to a correlation detector, contrary to a RAKE receiver that usually seeks a limited number of dominant paths.

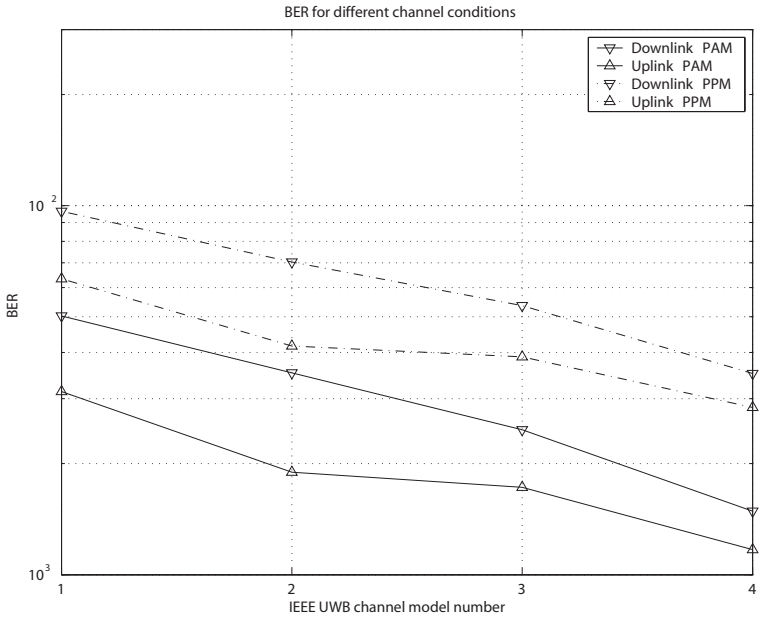

Figure 10: Effect of different communication channels on BER.

6 Conclusions

Incorporating PN sequences, multiuser transmitted reference (MTR) schemes are proposed for both PAM and PPM UWB systems. To obtain a satisfactory template for each correlation detector, a mean-based waveform estimation method is derived. Detailed analyses of waveform estimators and detector BERs are provided for various communication scenarios including uplink and downlink with both PAM and PPM. All analytical results are confirmed by experiments. Simulation results also demonstrate that the proposed detectors substantially outperform conventional TR detectors since they utilize significantly improved correlation templates. PAM signaling is slightly advantageous compared to PPM. Aided by PN sequences, multiuser communication is enabled, leading to large system capacity; the proposed systems can support many users at a reasonable raw BER level, while almost doubling the data rate of a conventional TR system.

References

[1] Federal Communications Commission News Release, "Revision of Part 15 of the Commission's Rules Regarding Ultra-Wideband Transmission Systems," ET Docket 98-153, Washington D.C., February 14, 2002.

[2] Qiu, R. C.; Liu, H.; Shen, X. Ultra-wideband for multiple access communications. *IEEE Commun. Magazine* **2005**, *43* (2), 80–87.

[3] Roy, S.; Foerester, J. R.; Somayazulu, V. S.; Leeper, D. G. Ultrawideband radio design: the promise of high-speed, short-range wireless connectivity. *Proc. of the IEEE* **2004**, *92* (2), 295–311.

[4] Yang, L.; Giannakis, G. B. Ultra-wideband communications: an idea whose time has come. *IEEE Sig. Proc. Magazine* **2004**, *21* (6), 26–54.

[5] Scholtz, R. A. Multiple access with time-hopping impulse modulation. *Proc. MILCOM'93*, October 1993, pp. 447–450.

[6] Hamalainen, M.; Hovinen, V.; Tesi, R.; Iinatti, J. H.; Latva-aho, M. On the UWB system coexistence with GSM900, UMTS/WCDMA, and GPS. *IEEE J. Selected Areas Commun.* **2002**, *20* (9), 1712–1721.

[7] Win, M.; Scholtz, R. Ultra-wide bandwidth time-hopping spread-spectrum impulse radio for wireless multiple-access communications. *IEEE Trans. Commun.* **2000**, *48* (4), 679–689.

[8] Barrett, T. W. History of ultra wideband communications and radar: Part I, UWB communications. *Microw. J.* **2001**, 22–56.

[9] Fontana, R. J.; Larrick, J. F.; Cade, J. E. 'An ultra-wideband communication link for unmanned vehicle applications. *Proc. 1997 AUVSI*, 1997.

[10] Win, M. Z.; Scholtz, R. A. On the energy capture of ultrawide bandwidth signals in dense multipath environments. *IEEE Commun. Letters*, **1998**, *2* (9), 245–247.

[11] Ramirez-Mireles, F. Performance of ultrawideband SSMA using time hopping and M-ary PPM. *IEEE J. Selected Areas Commun.* **2001**, *19* (6), 1186–1196.

[12] Taha, A.; Chugg, K. Multipath diversity reception of wireless multiple access time-hopping impulse radio. *Proc. 2002 UWBST* May 2002, pp. 283–288.

[13] Taylor, J. D. *Ultra-Wideband Radar Technology*, New York: CRC Press, 2001.

[14] Pausini, M.; Janssen, G. J. M. Analysis and comparison of autocorrelation receivers for IR-UWB signals based on differential detection. *Proc. of ICASSP* **2004**, *4*, 513–516.

[15] Guo, N.; Qiu, R. Improved autocorrelation receivers based on multiple symbol differential detection for UWB communications. IEEE Trans. Wireless Commun. **2005** (accepted).

[16] Xu, Z.; Tang, J.; Liu, P. Multiuser channel estimation for ultra-wideband systems using up to the second order statistics. *EURASIP Journal on Applied Signal Processing* **2004** (in press).

[17] Liu, P.; Xu, Z. POR-based channel estimation for UWB systems. *IEEE Trans. Wireless Commun.* **2005** (in press).

[18] Hocker, R. T.; Tomlinson, H. W. *An overview of Delay-hopped transmitted reference RF communications*; General Electronic Technical Report, 2001CRD198, Class 1, January 2002.

[19] Hocker, R. T.; Tomlinson, H. W. Delay-hopped transmitted reference RF communications. *Proc. 2002 UWBST* May 2002, pp. 265-270.

[20] Choi, J. D.; Stark, W. E. Performance of ultra-wideband communications with suboptimal receivers in multipath channels. *IEEE JSAC* **2002**, *20* (9), 1754–1766.

[21] Franz, S.; Mitra, U. On Optimal Data Detection for UWB Transmitted Reference Systems. *Proc. IEEE Globecom* **2003**, *2*, 744–748, San Francisco, CA.

[22] Rushforth, C. K. Transmitted-reference techniques for random or unknown channels. *IEEE Trans. Info. Theory* **1964**, *10* (1), 39–42.

[23] Gagliardi, R. A geometrical study of transmitted reference communication systems. *IEEE Trans. on Commun.* **1964**, *12* (4), 118–123.

[24] Hingorani, G. D.; Hancock, J. C. A transmitted reference system for communication in random or unknown channels. *IEEE Trans. Commun.* **1965**, *13* (3), 293–301.

[25] Chao, Y.; Scholtz, R. "Optimal and Suboptimal Receivers for Ultra-wideband Tranmitted Reference Systems," *Proc. IEEE Globecom* **2003**, *2*, 759–763, San Francisco, CA.

[26] http://grouper.ieee.org/groups/802/15, "Channel modeling subcommittee report final," Nov. 2002, IEEE P802.15-02/368r5-SG3a. Available: http://ieee802.org/15/pub/TG3.html

[27] Xu, Z.; Sadler, B.; Tang, J. Data Detection for UWB Transmitted Reference Systems with Inter-Pulse Interference. *Proc. of ICASSP*, Philadelphia, PA, March 19–23, 2005.

[28] Tang, J.; Xu, Z. Multidimensional Orthogonal Design for Ultra-Wideband Downlink. *Proc. of ICASSP*, Quebec, Canada, May 17-21, 2004.

[29] Le Martret, C. J.; Giannakis, G. B. All-digital impulse radio with multiuser detection for wireless cellular systems. *IEEE Trans. Commun.* **2002**, *50* (9), 1440–1450.

[30] Sari, H.; Vanhaverbeke, F.; Moeneclaey, M. Extending the capacity of multiple access channels. *IEEE Commun. Mag.* **2000**, 74–82.

[31] Vanhaverbeke, F.; Moeneclaey, M.; Sari, H. DS/CDMA with two sets of orthogonal spreading sequences and iterative detection. *IEEE Commun. Letters* **2000**, *4* (9), 289–291.

[32] Sadler, B. M.; Swami, A. On the performance of episodic UWB and direct-sequence communication systems. *IEEE Trans. Wireless Commun.* **2004**, *3* (6), 2246–2255.

[33] http://grouper.ieee.org/groups/802/15, "Channel modeling subcommittee report final," Nov. 2002, IEEE P802.15-02/368r5-SG3a.

[34] Xu, Z. Low complexity multiuser channel estimation with aperiodic spreading codes *IEEE Trans. Signal Processing*, **2001** *49* (11), 2813–28227.

A Optimization of the SINR

A.1 Proof of (32)

Power ϵ_n involves $E\{u_{k,m}(t)u_{k,m}(\tau)\}$. One may wonder if cross term $\delta h_k(t+a)\delta h_l(\tau+a)$ with $a = c_{k,m}T_c$ for $k \neq l$ plays an role. Towards this end, we express $\delta h_k(t+a)$ explicitly as

$$\begin{aligned}\delta h_k(t+a) &= \frac{1}{N_p}\sum_{m'} A_{l,m'}A_{k,m'}h_l(t+a) + \frac{1}{N_p}\sum_{m'}\sum_{l',l'\neq l,l'\neq k} A_{l',m'}A_{k,m'}h_{l'}(t+a) \\ &+ \frac{1}{N_p}\sum_{l',m'} A_{k,m'}B_{l',m'}I_{l',\lfloor m'/N_f\rfloor}h_{l'}(t+a-c_{l',m'}T_c) \\ &+ \frac{1}{N_p}\sum_{m'} A_{k,m'}v_{m'}(t+a) \end{aligned} \tag{A.1}$$

according to (14), similarly for $\delta h_l(t+a)$

$$\begin{aligned}\delta h_l(t+a) &= \frac{1}{N_p}\sum_{m'} A_{k,m'}A_{l,m'}h_k(t+a) + \frac{1}{N_p}\sum_{m'}\sum_{l',l'\neq l,l'\neq k} A_{l',m'}A_{l,m'}h_{l'}(t+a) \\ &+ \frac{1}{N_p}\sum_{l',m'} A_{l,m'}B_{l',m'}I_{l',\lfloor m'/N_f\rfloor}h_{l'}(t+a-c_{l',m'}T_c) \\ &+ \frac{1}{N_p}\sum_{m'} A_{l,m'}v_{m'}(t+a). \end{aligned} \tag{A.2}$$

Considering $A_{k,m}$ and $A_{l,m}$ are zero mean and independent, cross term has no effect on $E\{u_{k,m}(t)u_{k,m}(\tau)\}$. Therefore,

$$\begin{aligned}E\{u_{k,m}(t)u_{k,m}(\tau)\} &= \sum_l E\{\delta h_l(t+c_{l,m}T_c)\delta h_l(\tau+c_{l,m}T_c)\} + \sigma_v^2\phi(t-\tau) \\ &+ \sum_{l,l\neq k} h_l(t+c_{k,m}T_c-c_{l,m}T_c)h_l(\tau+c_{k,m}T_c-c_{l,m}T_c). \end{aligned} \tag{A.3}$$

Applying (15), it becomes

$$\begin{aligned}E\{u_{k,m}(t)u_{k,m}(\tau)\} &= \frac{1}{N_p}\sum_{l_1}\sum_{l_2,l_2\neq l_1} h_{l_2}(t+c_{l_1,m}T_c)h_{l_2}(\tau+c_{l_1,m}T_c) + (1+\frac{K}{N_p})\sigma_v^2\phi(t-\tau) \\ &+ \frac{1}{N_p^2}\sum_{l_1,l_2,m'} h_{l_2}(t+c_{l_1,m}T_c-c_{l_2,m'}T_c)h_{l_2}(\tau+c_{l_1,m}T_c-c_{l_2,m'}T_c) \\ &+ \sum_{l,l\neq k} h_l(t+c_{k,m}T_c-c_{l,m}T_c)h_l(\tau+c_{k,m}T_c-c_{l,m}T_c). \end{aligned} \tag{A.4}$$

Substituting (A.4) and (15) into (23), the interference plus noise power becomes

$$\begin{aligned}
\epsilon_n &= \sum_{l,l\neq k}\frac{\mathcal{E}^2_{k,l,0,0}}{N_p}+(\frac{\sigma_v^2}{N_f}+\frac{\sigma_v^2}{N_p}+\frac{\sigma_v^2 K}{N_f N_p})\mathcal{H}_{k,0}+\sum_{l,m'}\frac{\mathcal{E}^2_{k,l,0,c_{l,m'}}}{N_p^2}\\
&+ \sum_{l_1,m}\sum_{l_2,l_2\neq l_1}\frac{\mathcal{E}^2_{k,l_2,0,-c_{l_1,m}}}{N_f^2 N_p}+\sum_{l_1,l_2,m,m'}\frac{\mathcal{E}^2_{k,l_2,0,c_{l_2,m'}-c_{l_1,m}}}{N_f^2 N_p^2}+\sum_m\sum_{l,l\neq k}\frac{\mathcal{E}^2_{k,l,0,c_{l,m}-c_{k,m}}}{N_f^2}\\
&+ \sum_{l,l\neq k}\frac{\sigma_v^2}{N_f N_p}\mathcal{H}_{l,0}+\frac{\sigma_v^4}{N_f N_p}\mathcal{Y}+\sum_{l,m'}\frac{\sigma_v^2}{N_f N_p^2}\mathcal{H}_{l,c_{l,m'}}+\sum_m\sum_{l_1,l_2,l_1\neq k,l_2\neq k}\frac{\mathcal{E}^2_{l_1,l_2,0,c_{l_2,m}-c_{k,m}}}{N_f^2 N_p}\\
&+ \sum_m\sum_{l,l\neq k}\frac{\sigma_v^2}{N_f^2 N_p}\mathcal{H}_{l,c_{l,m}-c_{k,m}}+\sum_{l_1,m,m'}\sum_{l_2,l_2\neq k}\frac{\mathcal{E}^2_{l_1,l_2,c_{l_1,m'},c_{l_2,m}-c_{k,m}}}{N_f^2 N_p^2}. \qquad \text{(A.5)}
\end{aligned}$$

If all hopping sequences are periodic, then it reduces to (32).

A.2 Proof of (43)

From the expression of z_n, we obtain

$$\begin{aligned}
\epsilon_n &= \iint_0^{T_f} E\{\delta\Psi_{k,0}(t)\delta\Psi_{k,0}(\tau)\}h_k(t)h_k(\tau)dt\,d\tau\\
&+ \frac{1}{N_f^2}\sum_m\iint_0^{T_f}\Psi_{k,0}(t)\Psi_{k,0}(\tau)E\{u_{k,m}(t)u_{k,m}(\tau)\}dt\,d\tau\\
&+ \frac{1}{N_f^2}\sum_m\iint_0^{T_f}E\{\delta\Psi_{k,0}(t)\delta\Psi_{k,0}(\tau)\}E\{u_{k,m}(t)u_{k,m}(\tau)\}dt\,d\tau. \qquad \text{(A.6)}
\end{aligned}$$

It requires statistics of PPM template estimation error $\delta\Psi_{k,0}(t)$ and $u_{k,m}(t)$. According to (34), we have

$$\begin{aligned}
E\{\delta\Psi_{k,0}(t)\delta\Psi_{k,0}(\tau)\} &= \frac{1}{N_p}\sum_{l,l\neq k}\Psi_{l,0}(t)\Psi_{l,0}(\tau)\\
&+ \frac{\sigma_v^2}{N_p}\Big[2\phi(t-\tau)-\phi(t-\tau+\alpha T_c)-\phi(t-\tau-\alpha T_c)\Big]\\
&+ \frac{1}{2N_p^2}\sum_{i,l,m'}[h_l(t-c_{l,m'}T_c-i\alpha T_c)-h_l(t-c_{l,m'}T_c-(i+1)\alpha T_c)]\\
&\quad\times[h_l(\tau-c_{l,m'}T_c-i\alpha T_c)-h_l(\tau-c_{l,m'}T_c-(i+1)\alpha T_c)]. \qquad \text{(A.7)}
\end{aligned}$$

From (40), we find statistics of $u_{k,m}(t)$

$$\begin{aligned} E\{u_{k,m}(t)u_{k,m}(\tau)\} &= E\{\delta h_k(t+c_{k,m}T_c)\delta h_k(\tau+c_{k,m}T_c)\}+\sigma_v^2\phi(t-\tau) \\ &+ \sum_{l,l\neq k} h_l(t+c_{k,m}T_c)h_l(\tau+c_{k,m}T_c) \\ &+ \frac{1}{2}\sum_i\sum_{l,l\neq k} h_l(t+c_{k,m}T_c-c_{l,m}T_c-i\alpha T_c) \\ &\times h_l(\tau+c_{k,m}T_c-c_{l,m}T_c-i\alpha T_c). \end{aligned} \tag{A.8}$$

Applying (35), it becomes

$$\begin{aligned} E\{u_{k,m}(t)u_{k,m}(\tau)\} &= (1+\frac{1}{N_p})\sum_{l,l\neq k} h_l(t+c_{k,m}T_c)h_l(\tau+c_{k,m}T_c)+(1+\frac{1}{N_p})\sigma_v^2\phi(t-\tau) \\ &+\frac{1}{2N_p^2}\sum_{i,l,m'} \\ &\times h_l(t+c_{k,m}T_c-c_{l,m'}T_c-i\alpha T_c)h_l(\tau+c_{k,m}T_c-c_{l,m'}T_c-i\alpha T_c) \\ &+\frac{1}{2}\sum_i\sum_{l,l\neq k} \\ &\times h_l(t+c_{k,m}T_c-c_{l,m}T_c-i\alpha T_c)h_l(\tau+c_{k,m}T_c-c_{l,m}T_c-i\alpha T_c). \end{aligned} \tag{A.9}$$

Substituting (A.7) and (A.9) into (A.6), the interference plus noise power becomes

$$\begin{aligned} \epsilon_n = &\sum_{l,l\neq k}\frac{\mathcal{F}^2_{k,l,0,0}}{N_p}+\frac{\sigma_v^2}{N_p}\mathcal{R}_{k,0}+\sum_{i,l,m'}\frac{\mathcal{F}^2_{k,l,0,c_{l,m'}+i\alpha}}{2N_p^2}+\sum_m\sum_{l,l\neq k}\frac{1}{N_f^2}(1+\frac{1}{N_p})\mathcal{F}^2_{l,k,-c_{k,m},0} \\ &+(\frac{\sigma_v^2}{N_f}+\frac{\sigma_v^2}{N_fN_p})\mathcal{Q}_{k,0}+\sum_{i,l,m,m'}\frac{\mathcal{F}^2_{l,k,c_{l,m'}-c_{k,m}+i\alpha,0}}{2N_f^2N_p^2}+\sum_{i,m}\sum_{l,l\neq k}\frac{\mathcal{F}^2_{l,k,c_{l,m}-c_{k,m}+i\alpha,0}}{2N_f^2} \\ &+\sum_m\sum_{l_1,l_2,l_1\neq k,l_2\neq k}\frac{\mathcal{F}^2_{l_1,l_2,-c_{k,m},0}}{N_f^2N_p}+\sum_{l,l\neq k}\frac{\sigma_v^2}{N_fN_p}\mathcal{Q}_{l,0}+\sum_{i,m}\sum_{l_1,l_2,l_1\neq k,l_2\neq k}\frac{\mathcal{F}^2_{l_1,l_2,c_{l_1,m}-c_{k,m}+i\alpha,0}}{2N_f^2N_p} \\ &+\sum_m\sum_{l,l\neq k}\frac{\sigma_v^2}{N_f^2N_p}\mathcal{R}_{l,-c_{k,m}}+\frac{\sigma_v^4}{N_fN_p}\mathcal{X}+\sum_{i,m}\sum_{l,l\neq k}\frac{\sigma_v^2}{2N_f^2N_p}\mathcal{R}_{l,c_{l,m}-c_{k,m}+i\alpha} \\ &+\sum_{i,l_2,m,m'}\sum_{l_1,l_1\neq k}\frac{\mathcal{F}^2_{l_1,l_2,-c_{k,m},c_{l_2,m'}+i\alpha}}{2N_f^2N_p^2}+\sum_{i,l,m'}\frac{\sigma_v^2}{2N_fN_p^2}\mathcal{Q}_{l,c_{l,m'}+i\alpha} \\ &+\sum_{i_1,i_2,l_2,m,m'}\sum_{l_1,l_1\neq k}\frac{\mathcal{F}^2_{l_1,l_2,c_{l_1,m}-c_{k,m}+i_1\alpha,c_{l_2,m'}+i_2\alpha}}{4N_f^2N_p^2} \end{aligned} \tag{A.10}$$

where all terms of order $\frac{1}{N_p^2}$ in simplifying the third term of (A.6) have been ignored. If all hopping sequences are periodic, then it reduces to (43).

A.3 Proof of (48)

According to (47), we obtain

$$E\{u_{k,m}(t)u_{k,m}(\tau)\} = \sum_{l} E\{\delta h_l(t+c_{l,m}T_c)\delta h_l(\tau+c_{l,m}T_c)\} + \sigma_v^2\phi(t-\tau)$$
$$+\frac{1}{2}\sum_{l,l\neq k}\sum_{i} h_l(t+c_{k,m}T_c-c_{l,m}T_c-i\alpha T_c)h_l(\tau+c_{k,m}T_c-c_{l,m}T_c-i\alpha T_c). \quad \text{(A.11)}$$

Applying (35), it becomes

$$E\{u_{k,m}(t)u_{k,m}(\tau)\} = \frac{1}{N_p}\sum_{l_1}\sum_{l_2,l_2\neq l_1} h_{l_2}(t+c_{l_1,m}T_c)h_{l_2}(\tau+c_{l_1,m}T_c) + (1+\frac{K}{N_p})\sigma_v^2\phi(t-\tau)$$
$$+\frac{1}{2N_p^2}\sum_{i,l_1,l_2,m'} h_{l_2}(t+c_{l_1,m}T_c-c_{l_2,m'}T_c-i\alpha T_c)h_{l_2}(\tau+c_{l_1,m}T_c-c_{l_2,m'}T_c-i\alpha T_c)$$
$$+\frac{1}{2}\sum_{l,l\neq k}\sum_{i} h_l(t+c_{k,m}T_c-c_{l,m}T_c-i\alpha T_c)h_l(\tau+c_{k,m}T_c-c_{l,m}T_c-i\alpha T_c). \quad \text{(A.12)}$$

Substituting (A.7) and (A.12) into (A.6), the interference plus noise power becomes

$$\epsilon_n = \sum_{l,l\neq k}\frac{\mathcal{F}_{k,l,0,0}^2}{N_p} + \frac{\sigma_v^2}{N_p}\mathcal{R}_{k,0} + \sum_{i,l,m'}\frac{\mathcal{F}_{k,l,0,c_{l,m'}+i\alpha}^2}{2N_p^2} + \sum_{l_1,m}\sum_{l_2,l_2\neq l_1}\frac{\mathcal{F}_{l_2,k,-c_{l_1,m},0}^2}{N_f^2N_p} + (\frac{\sigma_v^2}{N_f}+\frac{\sigma_v^2K}{N_fN_p})\mathcal{Q}_{k,0}$$
$$+\sum_{i,l_1,l_2,m,m'}\frac{\mathcal{F}_{l_2,k,c_{l_2,m'}-c_{l_1,m}+i\alpha,0}^2}{2N_f^2N_p^2} + \sum_{i,m}\sum_{l,l\neq k}\frac{\mathcal{F}_{l,k,c_{l,m}-c_{k,m}+i\alpha,0}^2}{2N_f^2} + \sum_{l,l\neq k}\frac{\sigma_v^2}{N_fN_p}\mathcal{Q}_{l,0}$$
$$+\sum_{i,m}\sum_{l_1,l_2,l_1\neq k,l_2\neq k}\frac{\mathcal{F}_{l_1,l_2,c_{l_1,m}-c_{k,m}+i\alpha,0}^2}{2N_f^2N_p} + \frac{\sigma_v^4}{N_fN_p}\mathcal{X} + \sum_{i,m}\sum_{l,l\neq k}\frac{\sigma_v^2}{2N_f^2N_p}\mathcal{R}_{l,c_{l,m}-c_{k,m}+i\alpha}$$
$$+\sum_{i,l,m'}\frac{\sigma_v^2}{2N_fN_p^2}\mathcal{Q}_{l,c_{l,m'}+i\alpha} + \sum_{i_1,i_2,l_2,m,m'}\sum_{l_1,l_1\neq k}\frac{\mathcal{F}_{l_1,l_2,c_{l_1,m}-c_{k,m}+i_1\alpha,c_{l_2,m'}+i_2\alpha}^2}{4N_f^2N_p^2} \quad \text{(A.13)}$$

where all terms of order $\frac{1}{N_p^2}$ in simplifying the third term of (A.6) have been ignored, similarly as before. It reduces to (48) if periodic hopping sequences are employed.

Distribution

ADMNSTR
DEFNS TECHL INFO CTR
ATTN DTIC-OCP (ELECTRONIC COPY)
8725 JOHN J KINGMAN RD STE 0944
FT BELVOIR VA 22060-6218

DARPA
ATTN IXO S WELBY
3701 N FAIRFAX DR
ARLINGTON VA 22203-1714

OFC OF THE SECY OF DEFNS
ATTN ODDRE (R&AT)
THE PENTAGON
WASHINGTON DC 20301-3080

US ARMY TRADOC
BATTLE LAB INTEGRATION & TECHL DIRCTRT
ATTN ATCD-B
10 WHISTLER LANE
FT MONROE VA 23651-5850

SMC/GPA
2420 VELA WAY STE 1866
EL SEGUNDO CA 90245-4659

US ARMY ARDEC
ATTN AMSTA-AR-TD
BLDG 1
PICATINNY ARSENAL NJ 07806-5000

COMMANDING GENERAL
US ARMY AVN & MIS CMND
ATTN AMSAM-RD W C MCCORKLE
REDSTONE ARSENAL AL 35898-5000

US ARMY INFO SYS ENGRG CMND
ATTN AMSEL-IE-TD F JENIA
FT HUACHUCA AZ 85613-5300

US ARMY SIMULATION TRAIN & INSTRMNTN CMND
ATTN AMSTI-CG M MACEDONIA
12350 RESEARCH PARKWAY
ORLANDO FL 32826-3726

US GOVERNMENT PRINT OFF
DEPOSITORY RECEIVING SECTION
ATTN MAIL STOP IDAD J TATE
732 NORTH CAPITOL ST., NW
WASHINGTON DC 20402

UNIVERSITY OF CALIFORNIA, RIVERSIDE
DEPT OF ELECTRICAL ENGINEERING
ATTN Z XU
900 UNIVERSITY AVE
RIVERSIDE CA 92521

US ARMY RSRCH LAB
ATTN AMSRD-ARL-CI-OK-TP TECHL LIB T LANDFRIED (2 COPIES)
ABERDEEN PROVING GROUND MD 21005-5066

DIRECTOR
US ARMY RSRCH LAB
ATTN AMSRD-ARL-RO-EN W D BACH
PO BOX 12211
RESEARCH TRIANGLE PARK NC 27709

US ARMY RSRCH LAB
ATTN AMSRD-ARL-CI J GOWENS
ATTN AMSRD-ARL-CI-C W INGRAM
ATTN AMSRD-ARL-CI-CN A SWAMI
ATTN AMSRD-ARL-CI-CN B SADLER (5 COPIES)
ATTN AMSRD-ARL-CI-CN G RACINE (2 COPIES)
ATTN AMSRD-ARL-CI-CN S MISRA

ATTN AMSRD-ARL-CI-OK-T TECHL
PUB (2 COPIES)
ATTN AMSRD-ARL-CI-OK-TL TECHL
LIB (2 COPIES)
ATTN AMSRD-ARL-D J M MILLER
ATTN AMSRL-CI-CN T MOORE
ATTN IMNE-ALC-IMS MAIL &
RECORDS MGMT
ADELPHI MD 20783-1197